LAPPEENRANTA UNIVERSITY OF TECHNOLOGY

Department of Information Technology

Laboratory of Applied Mathematics

Paritosh R. Vasava

Fluid Flow in T-Junction of Pipes

The topic of this Master's thesis was approved by the department council of the Department of Information Technology on 16 January 2007.

The examiners of the thesis were Professor Heikki Haario and PhD Matti Heiliö. The thesis was supervised by PhD Matti Heiliö.

Lappeenranta, November 18, 2007

Paritosh R. Vasava

Teknologiapuistonkatu 4 C7

53850 Lappeenranta

+358 46 880 8245

vasava@lut.fi

ABSTRACT

Lappeenranta University of Technology
Department of Information Technology

Paritosh R Vasava

Fluid Flow in T-Junction of Pipes

Master's Thesis

2007

61 pages, 39 figures, 3 tables and 4 appendices

Examiners: Professor Heikki Haario

                        Dr Matti Heiliö

Keywords: T-junction, Head Loss, Navier-Stokes Equation, Kappa Epsilon model.

The aim of this work is to study flow properties at T-junction of pipe, pressure loss suffered by the flow after passing through T-junction and to study reliability of the classical engineering formulas used to find head loss for T-junction of pipes. In this we have compared our results with CFD software packages with classical formula and made an attempt to determine accuracy of the classical formulas. In this work we have studies head loss in T-junction of pipes with various inlet velocities, head loss in T-junction of pipes when the angle of the junction is slightly different from 90 degrees and T-junction with different area of cross-section of the main pipe and branch pipe.

In this work we have simulated the flow at T-junction of pipe with FLUENT and Comsol Multiphysics and observed flow properties inside the T-junction and studied the head loss suffered by fluid flow after passing through the junction. We have also compared pressure (head) losses obtained by classical formulas by A. Vazsonyi and Andrew Gardel and formulas obtained by assuming T-junction as combination of other pipe components and observations obtained from software experiments. One of the purposes of this study is also to study change in pressure loss with change in angle of T-junction.

Using software we can have better view of flow inside the junction and study turbulence, kinetic energy, pressure loss etc. Such simulations save a lot of time and can be performed without actually doing the experiment. There were no real life experiments made, the results obtained completely rely on accuracy of software and numerical methods used.

Acknowledgements

Contents

VOCABULARY

1-D   One Dimensional

2-D   Two Dimensional

3-D   Three Dimensional

N-D   N Dimensional (Where N is positive integer)

CFD   Computational Fluid Dynamics

NS   Navier-Stokes Equation

INS   Incompressible Navier-Stokes Equation

FDM   Finite Difference Method

FEM   Finite Element Method

FVM   Finite Volume Method

K-Epsilon   Kappa-Epsilon

NOTATIONS

Alphabetical Conventions

A	Pipe cross sectional area (cm^2)
C_μ	Constant used in mixing length turbulence model (Dimensionless)
$C_{1\epsilon}, C_{2\epsilon}$	Standard k-epsilon Model constants (Dimensionless)
D	Pipe diameter (cm)
d_h	Hydraulic diameter (cm)
e	Absolute roughness of pipe
e_l	Element of FEM domain
g	Acceleration due to gravity (cm^2/s) (g = 9.80665 cm^2/s)
g_i	Component of gravitational vector in the ith direction
H_l	Minor Loss Coefficient of pipe component (Dimensionless)
$K_{(i,j)}$	Loss-coefficient for flow coming from branch i to branch j
$k(x,t)$	turbulent kinetic energy
k	Relative roughness
l	Length of pipe (cm)
N_i	Node in element of FEM
r	Inner Pipe diameter (cm)
p	Pressure field
P_b	Effect of buoyancy
P_k	Production of k
P_{r_t}	Turbulent Prandtl number for energy ($P_{r_t} = 0.85$) [default value for standard K-epsilon models]
Q	Volumetric flow rate
r_p	Roughness coefficient of pipe material (dimensionless)
R_e	Reynolds numbers
S	modulus of the mean rate of strain tensor

U	Velocity vector field ($U = (u_1, u_2, u_3)$ each function of x and t)
u	x-component of velocity, (cm/s)
v	y-component of velocity (cm/s)
w	z-component of velocity, (cm/s)
$\bar{v}$	y-component of mean velocity cm/s
$\bar{u}$	x-component of mean velocity cm/s
$\bar{w}$	z-component of mean velocity cm/s

Greek Conventions

α	Angle in T-junction (for combining flow)
β, γ	Angles in T-junction (for dividing flow) [used in Chapter-4]
β	Coefficient of thermal expansion
τ	Shear Stress
η	Dynamic viscosity
λ	Friction Factor (dimensionless)
$\lambda_1, \lambda_2, \lambda_3$	Coefficients in Vazsonyi's formulas (dimensionless)
$\epsilon(x, t)$	Turbulent dissipation rate
μ	Fluid Viscosity, $Pa - s$
μ_t	Turbulent viscosity, $Pa - s$
σ	Symmetric stress tensor
σ_k	Turbulent Prandtl number for k
σ_ϵ	Turbulent Prandtl number for ϵ
ρ	Density of the fluid, g/cm^3
τ_ω	Shear stress, Pa
ς	Kinematic viscosity of fluid
θ	Angle between main pipe and branch

Mathematical Conventions

$\log(x)$	logarithm base 10 of x
e^x	exponential of x-that is, e raise to the power of x
$\sum_{i=1}^{n} a_i$	the sum from i=1 to n that is, $a_1 + a_2 + \ldots + a_n$
$\prod_{i=1}^{n} a_i$	the product from i=1 to n that is, $a_1 \times a_2 \times \ldots \times a_n$
$\partial f(x)/\partial x$	partial derivative of f with respect to x

$$\nabla = \left(\frac{\partial}{\partial x_1}, \ldots, \frac{\partial}{\partial x_n} \right) \quad \text{Vector differential operator (gradient)}$$

$$\Delta = \left(\frac{\partial^2}{\partial x_1^2}, \ldots, \frac{\partial^2}{\partial x_n^2} \right) \quad \text{Laplace operator (nabla)}$$

$$\Delta \cdot (c\nabla u) = \frac{\partial}{\partial x_1} \left(c \frac{\partial u}{\partial x_1} \right) + \ldots + \frac{\partial}{\partial x_n} \left(c \frac{\partial u}{\partial x_n} \right)$$

$$\beta \cdot \nabla u = \beta_1 \left(\frac{\partial u}{\partial x_1} \right) + \ldots + \beta_2 \left(\frac{\partial u}{\partial x_n} \right)$$

$\int_a^b f(x)$	the integral of f with respect to x
$F(x;\theta)$	function of x, with implied dependence upon θ

Mathematical Operations

$\equiv$	equivalent to (or defined to be)
$\propto$	proportional to

List of Figures

xi

List of Tables

1   Introduction

Pipe networks are mainly used for transportation and supply of fluids and gases. These networks vary from fewer pipes to thousands of pipes (e.g. water supply network of a large city, see in figure 1.1). In addition to pipes, the network also consists of elbows, T-junctions, bends, contractions, expansions, valves, meters, pumps, turbines and many other components. All these components cause loss in pressure due to change in momentum of the flow caused due to friction and pipe components. This means conversion of flow energy in to heat due to friction or energy lost due to turbulence.

Pipe networks are very common in industries, where fluid or gases are to be transported from one location to the other. The head loss (pressure loss) may vary depending on the type of components occurring in the network, material of the pipe and type of fluid transported through the network. In industries the networks are usually large and require very precise pressure at certain points of network. It is also sometimes essential to place valves, pumps or turbines of certain capacity to control pressure in the network. The placement of valves, pumps and turbines is important to overcome pressure loses caused by other components in the network. This is one of the important reasons why this study was conducted.
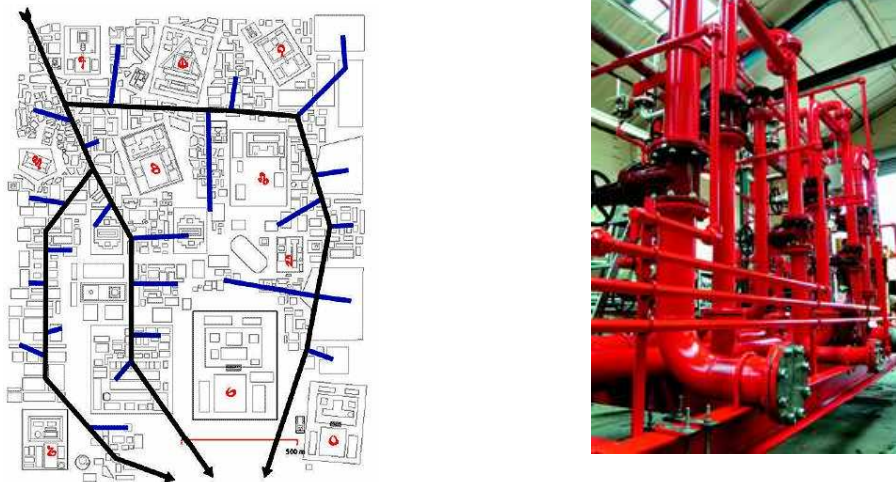
Figure 1.1: Water Distribution in city and industries.

In this work we have concentrated our attention to a very small and common component of pipe network: T-junction (Some also refer as 'Tee'). T-junction is a very common component in pipe networks, mainly used to distribute (diverge) the flow from main pipe

to several branching pipes and to accumulate (converge) flows from many pipes to a single main pipe. Depending on the inflow and outflow directions, the behavior of flow at the junction also changes. The following figure shows some possibilities of fluid entering and leaving the junction.
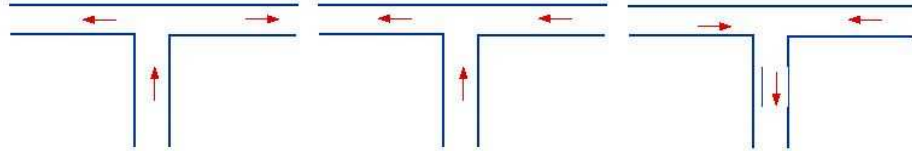
Figure 1.2: Various possibilities of fluid entering and leaving the junction

In present work we will numerically simulate the fluid flow in T-junction of pipes with Comsol Multiphysics and FLUENT. The results obtained by software were compared with available classical formula and formulas constructed by assuming T-junction to be made up of two different components. This comparison also helped in verification of some loss coefficients used in classical formula.

In fluid dynamics, **head** is the difference in elevation between two points in a column of fluid, and the resulting pressure of the fluid at the lower point. It is possible to express head in either units of height (e.g. meters) or in units of pressure such as Pascals. When considering a flow, one says that head is lost if energy is dissipated, usually through turbulence; equations such as the Darcy-Weisbach equation have been used to calculate the head loss due to friction.

Head losses are of two types major and minor. Major head losses (also called Frictional losses) are due to rough internal surface of pipe and occur over length of pipe. They are mainly due to friction. Minor losses are losses due to the change in fluid momentum. They are mainly due to pipe components due to bends, valves, sudden changes in pipe diameter, etc. Minor losses are usually negligible compared to friction losses in larger pipe systems. Presence of additional components offer resistance to flow and turbulence.

In this work, our aim is to study behavior of fluid at T-junction of pipes, head losses caused by T-junction and change in pressure loss with change in angle of the junction.

2 CFD tools used

In this chapter we present an assortment of mathematical methods that we have used in this study. This chapter includes overview of the CFD methods Finite Element method (FEM) and Finite Volume Method (FVM).

We begin this section with a small introduction to FEM. This will include overview and basic steps of FEM. Then, we will introduce FVM and also give basic steps of it.

2.1 Finite Element Method

The essence of the Finite Element Method (FEM) is to take a complex problem whose solution may be difficult if not impossible to obtain, and decompose it into pieces upon each of which a simple approximation of the solution may be constructed, and then put the local approximate solutions together to obtain a global approximate solution. FEM is widely used to find approximate solutions of differential equations which are not solvable with analytical methods or which have geometrically complex domains. There are commercial software packages like Comsol Multiphysics and ANSYS available for usage.

In FEM, we divide, domain $\Omega \in \Re^2$ of the boundary value problem into a number of closed sub-regions called elements ($\{e_l\}_{l=1}^{L}$). When we do this we take following precautions

1. Avoid very large and very small angles.

2. Element should be placed most densely in region where the solution of the problem and its expected to vary rapidly.

3. High accuracy requires a fine mesh or many nodes per element.

Suppose that for a given finite element mesh there is associated with each node $N_i = (x_i, y_i)$ a function, defined on $\bar{\Omega}$ with certain properties (see **appendix-C**), this function is called Elements basis functions. Local basis function over element e_l is simply the restriction of global element basis function of e_l.

This method involves simple steps as described briefly.

1. **Discretization of the domain**: Discretize the geometrically complex domain into set of finite elements called **elements**. We can divide the domain into desired number of elements and desired number of nodes. These elements are non-overlapping. It can be easily observed that the elements have simple geometrical form and are only part of the very complex looking geometry and nodes are the points where these elements meet. For 1-D the elements are intervals, for 2-D the elements are triangles or quadrilaterals.

2. **Weak formulation of the differential equation over elements**: Multiply the equation by a weight function and integrate the equation over the domain. Distribute the differentiation among the weight function. Use the definition of the natural boundary condition in the weak form.
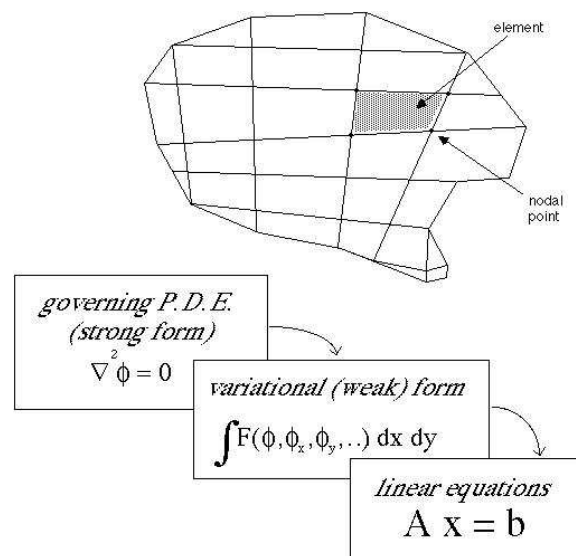
Figure 2.1: Finite Element Discretization of the domain and Weak formulation

3. **Local Approximation of Solution**: On each element let us attempt to compute the length. We assume that the length of each arc can be approximated by the length of the chord i.e. we approximate the arc using a straight line.

4. **Assemble the Element Equations**: Collect the element equations to get a representation of the whole system. Assemble the element equations to obtain the global system of equations.

5. **Imposition of boundary conditions**.

6. **Solution of the algebraic system of equations**: Obtain the Solution of standard matrix equation by direct or indirect (iterative) method.

7. **Post processing**: This final operation displays the solution to system equations in tabular graphical or pictorial form. Other meaningful quantities may be derived from the solution and also displayed.

The finite element solution converges to the true solution as the number of elements is increased. FEM is easy to use and it is also easy to approximate the differential terms of higher order. This method demands a good engineering judgment. The choice of type of element and other basis functions can be crucial.

2.2 Finite Volume Method

The Finite Volume Method (FVM) is a numerical method based on Integral conservation law. These methods are used for solving partial differential equations that calculates the values of the conserved variables averaged across the volume. The integral conservation law is enforced for small control volumes defined by the computational mesh. One advantage of FVM over FDMs is that it does not require a structured mesh (although a structured mesh can also be used). Furthermore, FVM is preferable to other methods as a result of the fact that boundary conditions can be applied non-invasively. This is true because the values of the conserved variables are located within the volume element, and not at nodes or surfaces. FVMs are especially powerful on coarse, non-uniform grids and in calculations where the mesh moves to track interfaces or shocks.

The FVMs are very efficient in solving conservative problems. They are extensively used in fluid mechanics and many other engineering areas governed by conservative systems that can be written in integral control volume form. The primary advantages of these methods are numerical robustness, applicability on very general unstructured meshes, and the intrinsic local conservation properties of the resulting schemes.

To use FVM concrete choice of control volumes, type of approximation inside them and numerical methods for evaluation of integrals and fluxes are required to be chosen carefully in advance. This method (Based on the control volume formulation of analytical fluid dynamics) involves simple steps as described briefly.

1. In FVM, computational domain is first tessellated into a collection of non overlap-

ping control volumes that completely cover the domain i.e. to divide the domain into a number of control volumes where the variable of interest is located at the centroid of the control volume. The control volumes are divided in to two categories: cell-centered and vertex-centered control volume (See fig 2.2) . In the cell-centered finite volume method shown, the triangles themselves serve as control volumes with solution unknowns (degrees of freedom) stored on a per triangle basis. In the vertex-centered finite volume method shown, control volumes are formed as a geometric dual to the triangle complex and solution unknowns stored on a per triangulation vertex basis. The following figures give clear idea about type of control volumes in 1D, 2D and 3D.
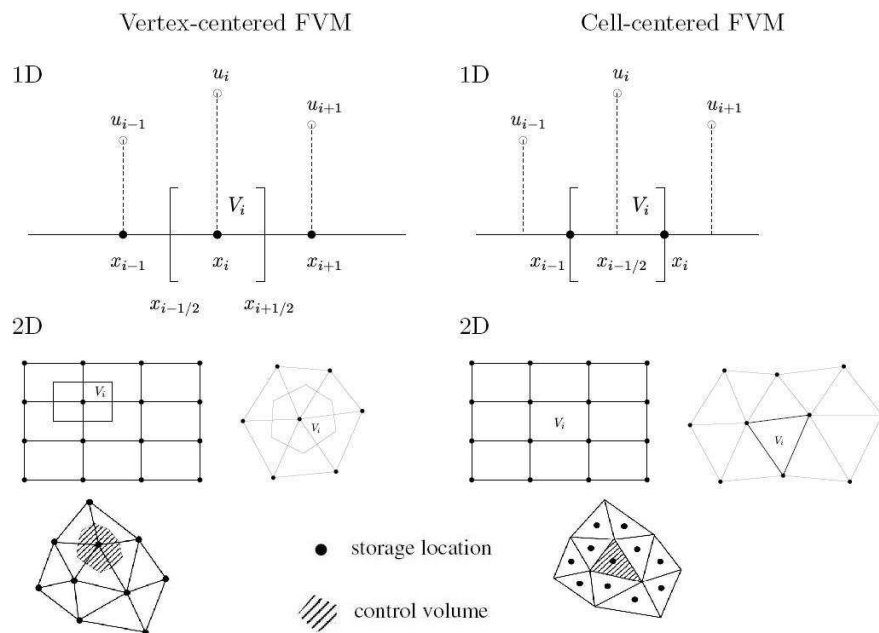
Figure 2.2: Control volume variants used in the finite volume method: cell-centered and vertex-centered control volume

2. Integrate the differential form of the governing equations (very similar to the control volume approach) over each control volume.

3. Interpolation profiles are then assumed in order to describe the variation of the concerned variable between cell centroids. The resulting equation is called the discretized or discretization equation. In this manner, the discretization equation expresses the conservation principle for the variable inside the control volume.

The most compelling feature of the FVM is that the resulting solution satisfies the conservation of quantities such as mass, momentum, energy, and species. This is exactly satisfied for any control volume as well as for the whole computational domain and for any number of control volumes. Even a coarse grid solution exhibits exact integral balances. FVM is the ideal method for computing discontinuous solutions arising in compressible flows. Any discontinuity must satisfy the Rankine-Hugoniot jump condition which is a consequence of conservation. Since FVMs are conservative they automatically satisfy the jump conditions and hence give physically correct weak solutions.

3 Governing Equations and Boundary Conditions

The flow of most fluids can be mathematically described by the use of continuity equation and momentum equation. According to continuity equation, the amount of fluid entering in certain volume leaves that volume or remains there and according to momentum equation tells about the balance of the momentum. The momentum equations are sometimes also referred as Navier-Stokes (NS) equation. They are most commonly used mathematical equations to describe flow. In this section we shall first derive NS equations and then K-Epsilon model. At the end we shall also briefly discuss boundary conditions used.

In this section, we shall derive Navier-Stokes equations by control volume method, the simplest approach. These equations can be used to describe many flow situations. Being second order, non-homogeneous, non-linear partial differential equations we require at least two boundary conditions for obtaining solution.

3.1 Continuity equation

Consider a volume of fluid in the stream with dimensions $\Delta x, \Delta y$ and Δz. Consider that the fluid flow is in positive x direction. Thus, the the amount of fluid that enters the volume from face-1 is equal to product of density (ρ), velocity of fluid in x-direction (u) and area of the face-1 ($\Delta y \Delta z$). Thus,

$$volume in_x = \rho u \Delta y \Delta z \tag{3.1}$$
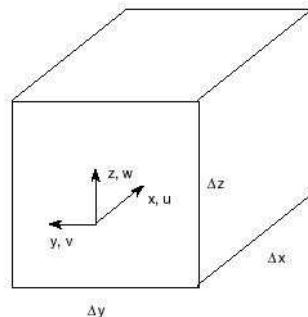
Figure 3.1: Elemental volume used to derive the equations

The mass leaving from face-2 is negative (its leaving the volume) product of density, velocity of fluid in x-direction and area of the face-2. But, the density and velocity of the fluid changes from u to $u + \Delta u$ and ρ to $\rho + \Delta\rho$. Thus,

$$volumeout_x = -(u + \Delta u)(\rho + \Delta\rho)u\Delta y\Delta z \tag{3.2}$$

Similarly, for other two faces parallel to y-axis, the equations for mass entering and leaving will be

$$volumein_y = \rho v\Delta x\Delta z \tag{3.3}$$

$$volumeout_y = -(v + \Delta v)(\rho + \Delta\rho)v\Delta x\Delta z \tag{3.4}$$

And, for other two faces parallel to z-axis, the equations for mass entering and leaving will be

$$volumein_z = \rho w\Delta x\Delta y \tag{3.5}$$

$$volumeout_z = -(w + \Delta w)(\rho + \Delta\rho)w\Delta x\Delta y \tag{3.6}$$

Also, the total amount of fluid accumulated in the volume $\Delta x\Delta y\Delta z$ is

$$\left(\frac{\Delta\rho}{\Delta t}\right)\Delta x\Delta y\Delta z \tag{3.7}$$

This amount must be equal to the numerical sum of all the terms representing fluid entering the volume and fluid leaving from the volume. Adding equations (3.1) to (3.7), equating to 0 and using $\Delta(fg) = f\Delta g + g\Delta f + \Delta f\Delta g$, we get

$$\left(\frac{\Delta\rho}{\Delta t}\right) = -\frac{(\Delta\,(\rho u))\,u\Delta y\Delta z - (\Delta\,(\rho v))\,v\Delta x\Delta z - (\Delta\,(\rho w))\,w\Delta x\Delta y}{\Delta x\Delta y\Delta z} \tag{3.8}$$

$$\Rightarrow \left(\frac{\Delta\rho}{\Delta t}\right) + \frac{\Delta(\rho u)}{\Delta x} + \frac{\Delta(\rho v)}{\Delta y} + \frac{\Delta(\rho z)}{\Delta z} \tag{3.9}$$

And when, $\Delta t \to 0$, we can replace Δ operator by partial differential operator.

$$\frac{\partial\rho}{\partial t} + \frac{\partial(\rho u)}{\partial x} + \frac{\partial(\rho v)}{\partial y} + \frac{\partial(\rho w)}{\partial z} = 0 \tag{3.10}$$

Which is general **Continuity equation** for compressible fluid. For incompressible fluids the Continuity Equation reduces to

$$\frac{\partial u}{\partial x} + \frac{\partial v}{\partial y} + \frac{\partial w}{\partial z} = 0 \tag{3.11}$$

Also, if the density ρ is a function of co-ordinates x, y and z but not time then,

$$\frac{\partial(\rho u)}{\partial x} + \frac{\partial(\rho v)}{\partial y} + \frac{\partial(\rho w)}{\partial z} = 0 \tag{3.12}$$

3.2 Navier-Stokes equation

Navier-Stokes (NS) equations are system of momentum equations for each co-ordinate directions. We shall derive the equation only for x co-ordinate and then write for y and z similarly. First we shall calculate Momentum Change and Flux and then calculate the forces.

3.2.1 Momentum Change and Flux

Consider a volume of fluid in the stream with dimensions $\Delta x, \Delta y$ and Δz. The change in momentum with respect to time is given by $\left(\partial(\rho u)/\partial t\right)\Delta x \Delta y \Delta z$.

The flux of momentum in the x direction at face-1 of the volume is the product of the mass flux (ρu), the x-direction velocity (u) and the area of face-1 ($\Delta y \Delta z$) i.e. $\rho u u \Delta y \Delta z$. The flux of momentum in the face opposite to face-1 is $-\left[\rho u u + (\partial(\rho u u))/\partial x \Delta x\right]\Delta y \Delta z$.

Similarly, for faces parallel to y-axis the flux of momentum in the y direction is $\rho v u \Delta x \Delta z$ and the flux of momentum in the opposite to face is $-\left[\rho v u + (\partial(\rho v u))/\partial y \Delta y\right]\Delta x \Delta z$.

And, for faces parallel to y-axis the flux of momentum in the z direction at entering face of the volume is $\rho w u \Delta x \Delta y$ and the flux of momentum in the opposite to face is $-\left[\rho w u + (\partial(\rho w u))/\partial z \Delta z\right]\Delta x \Delta y$. Adding all these terms and simplifying we get,

$$-\left[\frac{\partial(\rho u u)}{\partial x}\Delta x \Delta y \Delta z + \frac{\partial(\rho v u)}{\partial y}\Delta x \Delta y \Delta z + \frac{\partial(\rho w u)}{\partial z}\Delta x \Delta y \Delta z\right] \tag{3.13}$$

According to conservation of momentum law, algebraic sum of all these fluxes of momentum and the external forces at faces parallel to x-axis ($\sum F_x$) should be equal to change

10

in momentum in volume with respect to time i.e.

$$\frac{\partial(\rho u)}{\partial t}\Delta x\Delta y\Delta z = -\left[\frac{\partial(\rho uu)}{\partial x}\Delta x\Delta y\Delta z + \frac{\partial(\rho vu)}{\partial y}\Delta x\Delta y\Delta z + \frac{\partial(\rho wu)}{\partial z}\Delta x\Delta y\Delta z\right] + \sum F_x$$

(3.14)

Re-arranging , we get

$$\Rightarrow \left[\frac{\partial}{\partial t}(\rho u) + \frac{\partial(\rho uu)}{\partial x} + \frac{\partial(\rho vu)}{\partial y} + \frac{\partial(\rho wu)}{\partial z}\right]\Delta x\Delta y\Delta z = \sum F_x$$

(3.15)

Applying the derivative of product rule we get,

$$\left[\rho\frac{\partial u}{\partial t} + u\frac{\partial \rho}{\partial t} + u\frac{\partial(\rho u)}{\partial x} + \rho u\frac{\partial u}{\partial x} + v\frac{\partial(\rho u)}{\partial y} + \rho v\frac{\partial u}{\partial y} + w\frac{\partial(\rho u)}{\partial z} + \rho w\frac{\partial u}{\partial z}\right]\Delta x\Delta y\Delta z = \sum F_x$$

(3.16)

Rearranging the terms we get,

$$\left\{u\left[\frac{\partial \rho}{\partial t} + \frac{\partial(\rho u)}{\partial x} + \frac{\partial(\rho u)}{\partial y} + \frac{\partial(\rho u)}{\partial z}\right] + \rho\frac{\partial u}{\partial t} + \rho u\frac{\partial u}{\partial x} + \rho v\frac{\partial u}{\partial y} + \rho w\frac{\partial u}{\partial z}\right\}\Delta x\Delta y\Delta z = \sum F_x$$

(3.17)

The terms in square bracket sum up to zero because of equation of continuity. Thus, above equation reduces to momentum equation given below

$$\left\{\rho\frac{\partial u}{\partial t} + \rho u\frac{\partial u}{\partial x} + \rho v\frac{\partial u}{\partial y} + \rho w\frac{\partial u}{\partial z}\right\}\Delta x\Delta y\Delta z = \sum F_x$$

(3.18)

Similarly, we can obtain,

$$\left\{\rho\frac{\partial v}{\partial t} + \rho u\frac{\partial v}{\partial x} + \rho v\frac{\partial v}{\partial y} + \rho w\frac{\partial v}{\partial z}\right\}\Delta x\Delta y\Delta z = \sum F_y$$

(3.19)

and

$$\left\{\rho\frac{\partial w}{\partial t} + \rho u\frac{\partial w}{\partial x} + \rho v\frac{\partial w}{\partial y} + \rho w\frac{\partial w}{\partial z}\right\}\Delta x\Delta y\Delta z = \sum F_z$$

(3.20)

3.2.2 Calculating Forces

The external force $\sum F_x, \sum F_y$ and $\sum F_z$ which are external forces on the considered volume. These forces are of two types: Body forces (acting on volume) and surface forces (acting on surfaces).

Body forces are mostly due to gravitational forces acting on the fluid. The total body

force acting on the volume considered is the product of component of acceleration due to gravity in x-direction, mass of the fluid in the volume i.e.

$$g_x \rho \Delta x \Delta y \Delta z \tag{3.21}$$

Surface forces act on only one particular surface of the volume at a time, and arise due to pressure or viscous stresses. The stress on a surface of the control volume acts in the outward direction, and is given the symbol σ_{ij} with two subscripts. The first subscript i indicates the normal direction of the face on which the stress acts, while the second subscript j indicates the direction of the stress.

The force due to the stress is the product of the stress and the area over which it acts. Thus, on the faces with normals in the x-direction $(DyDz)$, the forces acting in the x-direction due to the direct stresses are $\sigma_{xx}\Delta y \Delta z$ and $\left\{\sigma_{xx} + \frac{\partial \sigma_{xx}}{\partial x}\Delta x\right\}\Delta y \Delta z$ Which sum to $\left\{\frac{\partial \sigma_{xx}}{\partial x}\right\}\Delta x \Delta y \Delta z$.

Similarly, on the faces with normals in the y-direction $(\Delta x \Delta z)$, the forces in the x-direction due to shear stresses sum to $\frac{\partial \sigma_{yx}}{\partial x}\Delta x \Delta y \Delta z$ and on the faces with normals in the z-direction $(\Delta x \Delta y)$, the forces in the x-direction due to shear stresses sum to $\left\{\frac{\partial \sigma_{zx}}{\partial x}\right\}\Delta x \Delta y \Delta z$.

The sum of all surface forces in the x-direction is thus

$$\left(\frac{\partial \sigma_{xx}}{\partial x} + \frac{\partial \sigma_{yx}}{\partial x} + \frac{\partial \sigma_{zx}}{\partial x}\right)\Delta x \Delta y \Delta z \tag{3.22}$$

The stress σ_{xx} includes the pressure p (negative sign because it is acting inward) and the normal viscous stress τ_{xx}. The stresses σ_{yx} and σ_{zx} include only viscous shearing stresses σ_{yx} and σ_{zx}. This gives the force in the x-direction as:

$$-\left(\frac{\partial p}{\partial x} + \frac{\partial \tau_{xx}}{\partial x} + \frac{\partial \tau_{yx}}{\partial y} + \frac{\partial \tau_{zx}}{\partial z}\right)\Delta x \Delta y \Delta z \tag{3.23}$$

3.2.3 Newtonian/Non-Newtonian Fluids

A Newtonian fluid is one whose stress at each point is linearly proportional to its strain rate at that point. The best example of this is water. A non-Newtonian fluid is one whose

viscosity changes with the applied strain rate. Thus, we can say that non-Newtonian fluids do not have a well-defined viscosity. The following figure can give a better idea of how fluids can be classified in Newtonian and other type of fluids.
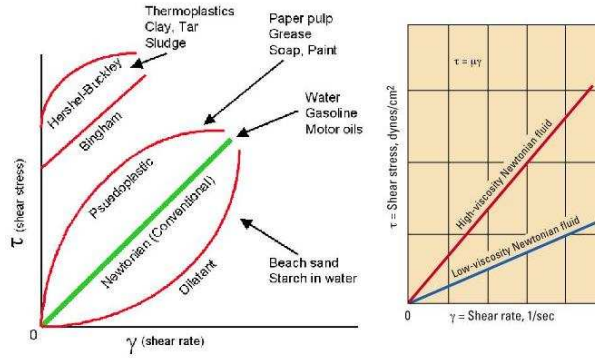
Figure 3.2: Fluid type Newtonian/conventional fluids vs. non-Newtonian fluids

A simple equation to describe Newtonian fluid behavior is $\tau = \mu \frac{du}{dx}$. In common terms, this means the fluid continues to flow, regardless of the forces acting on it. If the fluid is incompressible and viscosity is constant across the fluid, the equation governing the shear stress, in the Cartesian coordinate system, is

$$\tau_{ij} = \mu \left(\frac{dU_i}{dX_j} + \frac{dU_j}{dX_i} \right) \tag{3.24}$$

Where $U = (u, v, w)$ and $X = (x, y, z)$. Thus,

$$\tau_{xx} = \mu \left(\frac{du}{dx} + \frac{du}{dx} \right) = 2\mu \frac{du}{dx}, \tau_{yx} = \mu \left(\frac{dv}{dx} + \frac{du}{dy} \right), \tau_{zx} = \mu \left(\frac{dw}{dx} + \frac{du}{dz} \right) \tag{3.25}$$

Substituting these values in equation obtained above, we get,

$$-\left(\frac{\partial p}{\partial x} + \frac{\partial \left(2\mu \left(\frac{du}{dx} \right) \right)}{\partial x} + \frac{\partial \left(\mu \left(\frac{dv}{dx} + \frac{du}{dy} \right) \right)}{\partial y} + \frac{\partial \left(\mu \left(\frac{dw}{dx} + \frac{du}{dz} \right) \right)}{\partial z} \right) \Delta x \Delta y \Delta z \tag{3.26}$$

$$\Rightarrow -\left(\frac{\partial p}{\partial x} + 2\mu \frac{\partial^2 u}{\partial x^2} + \mu \left(\frac{\partial^2 u}{\partial y^2} + \frac{\partial \left(\frac{dv}{dx} \right)}{\partial y} + \frac{\partial^2 u}{\partial z^2} + \frac{\partial \left(\frac{dw}{dx} \right)}{\partial z} \right) \right) \Delta x \Delta y \Delta z \tag{3.27}$$

The terms $\partial^2 u/\partial x^2$, $\partial\left(dv/dx\right)/\partial y$ and $\partial\left(dw/dx\right)/\partial z$ cancel out due to continuity equation. The terms that remain along with the body force due to acceleration due to gravity would give the equation for the force in the x-direction,

$$\sum F_x = \left\{ \rho g_x - \frac{\partial p}{\partial x} + \mu \left(\frac{\partial^2 u}{\partial x^2} + \frac{\partial^2 u}{\partial y^2} + \frac{\partial^2 u}{\partial z^2} \right) \right\} \Delta x \Delta y \Delta z \qquad (3.28)$$

Substituting this in momentum equation, we get

$$\left\{ \rho \frac{\partial u}{\partial t} + \rho u \frac{\partial u}{\partial x} + \rho v \frac{\partial u}{\partial y} + \rho w \frac{\partial u}{\partial z} \right\} \Delta x \Delta y \Delta z = \rho g_x - \frac{\partial p}{\partial x} + \mu \left(\frac{\partial^2 u}{\partial x^2} + \frac{\partial^2 u}{\partial y^2} + \frac{\partial^2 u}{\partial z^2} \right)$$
$$(3.29)$$

Similarly, we can obtain,

$$\left\{ \rho \frac{\partial v}{\partial t} + \rho u \frac{\partial v}{\partial x} + \rho v \frac{\partial v}{\partial y} + \rho w \frac{\partial v}{\partial z} \right\} \Delta x \Delta y \Delta z = \rho g_y - \frac{\partial p}{\partial y} + \mu \left(\frac{\partial^2 v}{\partial x^2} + \frac{\partial^2 v}{\partial y^2} + \frac{\partial^2 v}{\partial z^2} \right)$$
$$(3.30)$$

and

$$\left\{ \rho \frac{\partial w}{\partial t} + \rho u \frac{\partial w}{\partial x} + \rho v \frac{\partial w}{\partial y} + \rho w \frac{\partial w}{\partial z} \right\} \Delta x \Delta y \Delta z = \rho g_z - \frac{\partial p}{\partial z} + \mu \left(\frac{\partial^2 w}{\partial x^2} + \frac{\partial^2 w}{\partial y^2} + \frac{\partial^2 w}{\partial z^2} \right)$$
$$(3.31)$$

These are the Navier-Stokes equations. There have been attempts to solve these equations but the computational complexity involved has not allowed many but some solutions. Navier-Stokes equation can be solved numerically, but the solutions are obtained after only making some assumptions and some of them are not stable at high Reynolds number.

There are two important issues that arise in the solution process first is non-linearity of the equations and second is the coupling of the equations. In CFD the stress tensor terms are often approximated by a turbulence model. The non-linearity makes most problems difficult or impossible to solve and is part of the cause of turbulence.

3.3 Turbulence

Dictionary meaning of turbulence is the state of being turbulent and turbulent means disturbed. When we talk about turbulence in fluid dynamics it means fluid flow with violent disorder where the disorder has no specific direction or pattern. Also, its quoted as a

random secondary motion caused by eddies with in the fluid in motion. Even though turbulence is an everyday experience, it is extremely difficult to find solutions, quantify, or in general characterize. When the flow is turbulent, we can expect a very rapid and random change in fluid and fluid motion properties like momentum diffusion, high momentum convection, variation of pressure and velocity in space and time. Its difficult to express turbulence mathematically for following reasons.

1. Irregularity or randomness: impossible to apply a deterministic approach.

2. Diffusivity: This characteristic causes rapid mixing and increased rate of momentum, heat and mass transfer.

3. Large Reynolds number: Turbulent flow or instable laminar flow.

4. 3D Vorticity fluctuations: Turbulence is 3D and rotational. Turbulence is characterized by high levels of fluctuating vorticity.

5. Dissipation: Turbulence flows are always dissipative. Viscous shear stress performs deformation work which increases the internal energy of the fluid at expense of kinetic energy of the turbulence. A continuous energy supply is needed to keep up these loses. If no energy is supplied turbulence decays rapidly.

The K-epsilon model is one of the most common turbulence models. It includes two transport equations to represent the turbulent properties of the flow. This allows a two equation model to account for history effects like convection and diffusion of turbulent energy. The first transported variable is turbulent kinetic energy (k). The second transported variable in this case is the turbulent dissipation (ϵ). These variables determine the scale of the turbulence and energy in the turbulence. In next part, we shall derive Kappa-Epsilon model from Incompressible NS equations.

3.4 Kappa-Epsilon Model

The K-epsilon model is most commonly used to describe the behavior of turbulent flows. It was proposed by A.N Kolmogrov in 1942, then modified by Harlow and Nakayama and produced K-Epsilon model for turbulence.

The Transport Equations for K-Epsilon model are For k,

$$\frac{\partial}{\partial t}(\rho k) + \frac{\partial}{\partial t}(\rho k u_i) = \frac{\partial}{\partial x_j}\left[\left(\mu + \frac{\mu_t}{\sigma_k}\right)\frac{\partial k}{\partial x_j}\right] + P_k + P_b - \rho\epsilon - Y_k + S_k \qquad (3.32)$$

For ϵ,

$$\frac{\partial}{\partial t}(\rho\epsilon) + \frac{\partial}{\partial t}(\rho\epsilon u_i) = \frac{\partial}{\partial x_j}\left[\left(\mu + \frac{\mu_t}{\sigma_k}\right)\frac{\partial\epsilon}{\partial x_j}\right] + C_{1\epsilon}\frac{\epsilon}{k}\left(P_k + C_{3\epsilon}P_b\right) - C_{2\epsilon}\rho\frac{\epsilon^2}{k} + S_\epsilon \qquad (3.33)$$

Realizable k-epsilon model and RNG k-epsilon model are some other variants of K-epsilon model. K-epsilon model has solution in some special cases. K-epsilon model is only useful in regions with turbulent, high Reynolds number flows.

3.5 Derivation

K-epsilon model equations can be derived form incompressible Navier stokes equation.

$$\rho(u.\nabla)u = \nabla\left\{-pI + \eta\left(\nabla u + (\nabla u)^T\right)\right\} + F \qquad (3.34)$$

$$\nabla.u = 0 \qquad (3.35)$$

Where, u is velocity vector field, p is pressure field, following are steps for deriving k-epsilon model.

1. Apply statistical averaging to NS equation (3.35)

$$\rho\left(\frac{\partial u_i}{\partial t} + \sum_j u_j\frac{\partial u_j}{\partial x_j}\right) = \frac{\partial p}{\partial x_i} + \eta\nabla_2 u_i \qquad (3.36)$$

Where, $u(x,t)$ represents the velocity vector field, $p(x,t)$ is the pressure field. Being derived from Equations of conservation of mass, momentum and energy, we have,

$$\frac{\partial\rho}{\partial t} + \sum_j u_j\frac{\partial\rho}{\partial x_j} = \sum_j u_j\frac{\partial u_j}{\partial x_j} = 0 \qquad (3.37)$$

Applying statistical averaging to equation (3.36) produces Reynolds equation:

$$\rho\frac{\partial\overline{u_i}}{\partial t} + \sum_j u_j\left(\rho\overline{u_j}\frac{\partial\overline{u_i}}{\partial x_j} + \rho\overline{\frac{\partial u_i'}{\partial x_j}u_j'}\right) = \frac{\partial\overline{p}}{\partial x_i} + \sum_j u_j\frac{\partial\overline{\tau_{ij}}}{\partial x_j} \qquad (3.38)$$

With $u = \overline{u} + u'$ written in the mean plus fluctuation decomposition, averaging satisfying the field rules (see **appendix C**) and using the following two equations.

$$\tau_{ij} = \eta \left(\frac{\partial \overline{u_i}}{\partial x_j} + \frac{\partial \overline{u_j}}{\partial x_i} \right)$$

$$\eta \nabla^2 u_i = \sum_j \frac{\partial \tau_{ij}}{\partial x_j}$$

2. Multiply Navier-Stokes (3.36) by u_i and average it.

$$\rho \overline{\frac{\partial u_i}{\partial t} u_i} + \rho \sum_j \overline{u_j \frac{\partial u_i}{\partial x_j} u_i} = -\overline{\frac{\partial p}{\partial x_i} u_i} + \sum_j \overline{\frac{\partial \tau_{ij}}{\partial x_j} u_i} \qquad (3.39)$$

3. Multiply obtained Reynolds equation (3.38) by $\overline{u_i}$.

$$\rho \frac{\partial \overline{u_i}}{\partial t} \overline{u_i} + \sum_j \left(\rho \overline{u_j} \frac{\partial \overline{u_i}}{\partial x_j} \overline{u_i} + \rho \overline{\frac{\partial u_i'}{\partial x_j} u_j'} \right) = -\frac{\partial \overline{p}}{\partial x_i} \overline{u_i} + \sum_j \frac{\partial \overline{\tau_{ij}}}{\partial x_j} \overline{u_i} \qquad (3.40)$$

Where,

$$\overline{\frac{\partial u_i'}{\partial x_j} u_j'} = \frac{\partial \left(\overline{u_i' u_j'} \right)}{\partial x_j}$$

or equivalently

$$\rho \overline{\frac{\partial u_i'}{\partial t} u_i'} + \rho \sum_j \overline{u_j} \frac{\partial \overline{u_i}}{\partial x_j} \overline{u_i} = -\frac{\partial \overline{p}}{\partial x_i} \overline{u_i} + \sum_j \left(\frac{\partial \tau_{ij}}{\partial x_j} \overline{u_i} + \frac{\partial T_{ij}}{\partial x_j} \overline{u_i} \right) \qquad (3.41)$$

With $T_{ij} = -\rho \overline{u_i' u_j'}$ representing the components of the Reynolds stress matrix T.

4. Subtracting equation ((3.39)) from equation ((3.41)), we get.

$$\rho \overline{\frac{\partial u_i'}{\partial t} u_i'} + \rho \sum_j \left(\overline{u_j \frac{\partial u_i}{\partial x_j} u_i} - \overline{u_j} \frac{\partial \overline{u_i}}{\partial x_j} \overline{u_i} \right) = -\overline{\frac{\partial p'}{\partial x_i} u_i'} + \sum_j \left(\overline{\frac{\partial \tau_{ij}'}{\partial x_j} u_i'} - \frac{\partial T_{ij}}{\partial x_j} \overline{ui} \right) \qquad (3.42)$$

Where,

$$\overline{\frac{\partial \tau_{ij}'}{\partial x_j} u_i'} = \frac{\partial (\overline{\tau_{ij}' u_i'})}{\partial x_j} - \overline{\frac{\partial u_i'}{\partial u_i} \tau_{ij}'}$$

5. Neglecting very small viscous transfer or turbulent energy, we get (3.43). Since, the $\tau_{ij}' u_i'$ represents the viscous transfer of turbulent energy, a very small quantity in contrast to the terms responsible for the turbulent energy in, it is neglected. Thus

17

becomes

$$\rho \overline{\frac{\partial \overline{u_i'}}{\partial t} u_i'} + \rho \sum_j \overline{u_i' \frac{\partial u_i'}{\partial x_j}} \overline{u_j} + \sum_j \left(\rho \overline{\frac{\partial \overline{u_i'}}{\partial x_j} u_i' u_j'} + \frac{\partial \overline{\rho u_i' u_j'}}{\partial x_j} \overline{u_i} + \rho \overline{u_j' u_i'} \frac{\partial u_i'}{\partial x_j} \right)$$
$$= -\overline{\frac{\partial p'}{\partial x_j} u_i'} - \sum_j \left(\overline{\frac{\partial u_i'}{\partial x_j} \tau_{ij}'} + \frac{\partial T_{ij}}{\partial x_j} \overline{u_i'} \right) \quad (3.43)$$

6. Summing over i equation (3.43) becomes energy balance equation of turbulent flow, with turbulent kinetic energy (K) and rate of dissipation of the turbulent energy (ϵ).

7. Using hypothesis for class of fluid flow under consideration the equation of turbulent energy balance reduces to For k,

$$\frac{\partial k}{\partial t} = \frac{\partial}{\partial t} \left(c_k \frac{\partial k}{\partial x} \right) - \epsilon \quad (3.44)$$

Where, c_k is turbulent exchange coefficient. For ϵ,

$$\frac{\partial \epsilon}{\partial t} = \frac{\partial}{\partial t} \left(C_\epsilon \frac{\partial \epsilon}{\partial x} \right) - U \quad (3.45)$$

Where, C_ϵ is turbulent energy dissipation rate exchange coefficient and S rate of homogenification of the dissipation rate and is > 0.

3.6   Initial condition and Boundary condition

There are number of boundary conditions that we will use to solve Incompressible Navier-Stokes Equation and Kappa-Epsilon model. The figure 3.6 shows an example how the boundary conditions could be applied. The boundary conditions have been listed below.

Inflow/Outflow boundary condition
For inlet, imposed velocity i.e. the velocity vector normal to the boundary can be specified by:
$$u \cdot n = u_0 = (u_0, v_0, w_0)$$

which is denoted as the Inflow/Outflow boundary condition. In the above equation **n** is a unit vector that has a direction perpendicular to a boundary or normal to a boundary.

Outflow/Pressure boundary condition
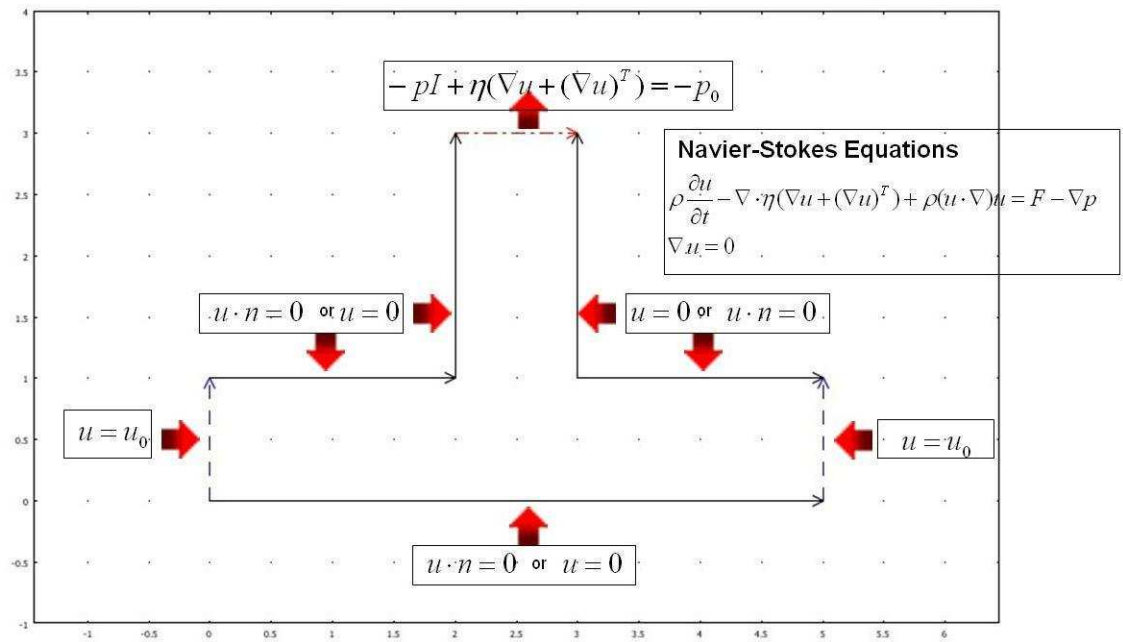
Figure 3.3: Use of boundary conditions with Comsol

For outlet, we can impose a certain pressure in the Outflow/Pressure boundary condition:

$$p = p_0$$

or

$$\left[-pI + \eta \left(\nabla u + (\nabla u)^T \right) \right] = -p_0$$

This is the Normal flow/Pressure boundary condition, which sets the velocity components in the tangential direction to zero, and sets the pressure to a specific value.

Slip/Symmetry boundary condition

The Slip/Symmetry condition states that there are no velocity components perpendicular to a boundary.

$$n \cdot u = 0$$

No slip boundary condition

The No-slip boundary condition eliminates all components of the velocity vector.

$$u = 0$$

Neutral boundary condition

The Neutral boundary condition states that transport by shear stresses is zero across a boundary. This boundary condition is denoted neutral since it does not put any constraints on the velocity and states that there are no interactions across the modeled boundary.

$$\eta \left(\nabla u + (\nabla u)^T \right) n = 0$$

The neutral boundary condition means that no forces act on the fluid and the computational domain extends to infinity.

4 Head losses

Head is a term used to specify measure of pressure of total energy per unit weight above a point of reference. In general, head is sum of three components; **elevation head** (the elevation of the point at which the pressure is measured from above or below the arbitrary horizontal observation point i.e. relative potential energy in terms of an elevation), **velocity head** (kinetic energy from the motion of water) (it is mainly used to determine minor losses) and **pressure head** (equivalent gauge pressure of a column of water at the base of the piezometer). [1]

In cases where the fluid is moving with very low velocity or stationary fluid, we ignore the velocity head because the fluid is either stationary or moving with very low velocity and in the cases where the fluid is moving with very high velocity (cases where the Reynolds's number exceeds 10) the elevation head and pressure head are neglected.

Head loss in fluid flow in pipes means loss of flow energy due to friction or due to turbulence. Head losses result in to loss in pressure at final outlet. The pressure loss is divided in two categories of Major (friction) losses and Minor losses. These losses are dependent on both the type of fluid and the material of the pipe.

Head loss is a measure to calculate reduction or loss in head. Head loss is mainly due to friction between fluid and walls of the duct (in our case it is pipe), friction between adjacent layers of fluid and turbulence caused by presence of pipe network components like T-junction, elbows, bends, contractions, expansions, pumps, valves. Head losses result in to loss in pressure at final outlet, thus also known as pressure loss. Pressure losses are divided in to two categories of major losses and minor losses.

- **Major losses**: Losses due to friction between fluid and internal pipe surface. These losses occur over the length of pipe. They can be easily determined by Darcy-Weisbach equation. Frictional loss is that part of the total head loss that occurs as the fluid flows through straight pipes

- **Minor losses**: Losses occur at points where there is change in momentum. They mainly occur at elbows, bends, contractions, expansions, valves, meters and similar other pipe fittings that commonly occur in pipe networks.

---

[1]A piezometer is small diameter water well used to measure the hydraulic head of underground water.

The major head loses may be large when the pipes are long (e.g. pipe network occurring in water distribution in a city) and minor losses will also have a large contribution because of attachments and fittings occurring in these networks. Thus, we can say that head loss in reality are unavoidable, since no pipes are perfectly smooth to have fluid flow without friction, there does not exist a fluid in which flows without turbulence.

The head loss for fluid flow is directly proportional to the length of pipe, the square of the fluid velocity, and a term accounting for fluid friction called the friction factor. The head loss is inversely proportional to the diameter of the pipe. Head loss is unavoidable in pipe networks with real fluids, since there is no pipe with perfectly smooth inner surface and there is no fluid that can flow without turbulence.
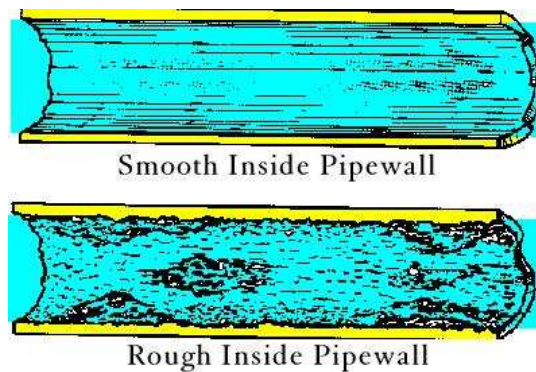
Figure 4.1: Fluid behavior when pipe is smooth or rough from inside

The calculation of the head loss depends on whether the flow is laminar, transient or turbulent and this we can determine by calculating Reynolds number.

4.1 Major head loss

There are many equations available to determine major head losses in a pipe. The most fundamental of all is Darcy-Weisbach Equation. Major head loss (loss due to friction) is determined by

$$h_{major} = \lambda \left(\frac{l}{d_h} \right) \left(\frac{\rho v^2}{2} \right)$$

This equation is valid for fully developed, steady, incompressible flow. The hydraulic diameter (d_h) is division on cross-section area of pipe by wetted perimeter.

$$d_h = \frac{cross\,section\,area\,of\,pipe}{wetted\,perimeter} = \frac{4\left(\pi r^2\right)}{2\pi r} = 2r = D$$

Thus, hydraulic diameter is the inner diameter of pipe. Therefore, major head loss formula reduces to

$$h_{major} = \lambda \left(\frac{l}{D}\right) \left(\frac{v^2}{2g}\right) \tag{4.1}$$

4.2 Friction Factor

Friction factor (λ) depends on whether the flow is laminar, transient or turbulent, which again depends on Reynolds number. **Friction Factor for Laminar Flow**
Consider

$$y = r - R \Rightarrow dy = -dr$$

and shearing stress

$$\tau = -\mu \frac{d\nu}{dr}$$

Where, ν is rate of change of velocity.

If we consider the fluid to be isolated from the surrounding, the inlet will have velocity (v_1) and pressure (p_1) and outlet will have velocity (v_2) and pressure (p_2).

Using momentum principle[2] (in fluid dynamics), we get

$$p_1 A - p_2 A + (shearing\,stress \times perimeter\,of\,pipe \times length\,of\,pipe) = \rho Q\left(v_2 - v_1\right)$$

$$\Rightarrow \left(p_1 - p_2\right) \pi r^2 - \tau(2\pi r L) = \rho Q\left(v_2 - v_1\right)$$

We know that

$$\tau = \frac{p_1 - p_2}{2L} \cdot r$$

and

$$\tau = -\mu \frac{d\nu}{dr}$$

---

[2]The principle of conservation of momentum is an application of Newton's second law of motion to an element of fluid. That is, when considering a given mass of fluid, it is stated that the rate at which the momentum of the fluid mass is changing is equal to the net external force acting on the mass.

Comparing both we get,

$$dv = -\frac{p_1 - p_2}{2L\mu} \cdot r\,dr$$

On integrating both sides and using $v = 0$ at $r = R$ and taking $p_1 - p_2 = \Delta p$, we get

$$v = -\frac{\Delta p}{2L\mu} \cdot \left(R^2 - r^2\right)$$

The volumetric flow (Q) can be determined by

$$Q = \int v\,(2\pi r)\,dr = \int_R^0 \frac{\Delta p}{2L\mu} \left(R^2 - r^2\right) (2\pi r)\,dr$$

$$\Rightarrow Q = \frac{\Delta p}{4L\mu}\pi r^4$$

And average velocity (V) can be determined by

$$V = \frac{Q}{A} = \frac{\Delta p}{4L\mu}\pi r^4 \cdot \frac{1}{\pi r^2}$$

$$\Rightarrow \Delta p = \frac{4L\mu}{R^2} \cdot V$$

Since, head loss equals pressure drop (Δp) divided by γ

$$h_{major} = \frac{\Delta p}{\gamma} = \frac{4L\mu}{\gamma R^2} \cdot V$$

Also,

$$h_{major} = \lambda \frac{L}{D} \cdot \frac{V^2}{2g}$$

Comparing both, we get

$$\lambda = \frac{64\frac{L}{D}}{VD} = \frac{64}{R_e}$$

Thus, $\lambda = \frac{64}{R_e}$ when $R_e < 2100$. This can also be confirmed from Nikuradse's graph for laminar flow. [3]

Friction Factor for Transient Flow

If the Reynolds number for the flow is between 2300 and 3000 the type of flow exhibited by the fluid is known as transient flow. This is type of flow where velocity and pressure of

---

[3]Nikuradse showed the dependence on roughness by using pipes artificially roughened by fixing a coating of uniform sand grains to the pipe walls. The degree of roughness was designated as the ratio of the sand grain diameter to the pipe diameter (ϵ/D).

the flow are changing with time. The flow also switches between turbulent and laminar. Because of this behavior it is difficult to determine the friction coefficient. Thus, the friction coefficient for Transient flow can not be determined.

Friction Factor for Turbulent Flow

When the flow is turbulent, the frictional factor (λ) can be obtained by solving the equation

$$\frac{1}{\sqrt{\lambda}} = -2.0 log_{10} \left[\frac{2.51}{R_e \sqrt{\lambda}} + \frac{r_p}{d_h} \cdot \frac{1}{3.72} \right]$$

Where, r_p is relative roughness of the pipe.

This equation is well known as Colebrooke equation[4]. Colebrooke equation is also graphically presented by Moody Chart[5], which can be easily used if some required parameter values are known. The Moody chart relates the friction factor for fully developed pipe flow to the Reynolds number and relative roughness of a circular pipe. Relative roughness for some common materials can be found in the table- 1[6] below.

Surface	Roughness (r_p) $\times 10^{-3}$ **m**
Copper, Lead, Brass, Aluminum (new)	$0.001 - 0.002$
PVC and Plastic Pipes	$0.0015 - 0.007$
Epoxy, Vinyl Ester and Isophthalic pipe	0.005
Stainless steel	0.015
Steel commercial pipe	$0.045 - 0.09$
Rusted steel (corrosion)	0.15
Smoothed cement	$0.3 - 1$
Ordinary concrete	$0.3 - 0.5$

Table 1: Relative roughness for some common materials determined by experiments.

Relative roughness of the pipe (r_p) can be easily determined if we know the material of the pipe. This value completely depends on material of pipe. These values are also easily available on some manuals. Table-2 summarizing relation between Reynolds number (R_e), the type of flow and Friction coefficient (λ)

The Friction coefficient (λ) can also be determined by Moody Chart. There is also a section in this chapter that briefly describes the use. An illustration is also given to understand

---

[4]The Colebrook equation is an implicit equation which combines experimental results of studies of laminar and turbulent flow in pipes. It was developed in 1939 by C. F. Colebrook.

[5]In 1944 Lewis F. Moody, Professor, Hydraulic Engineering, Princeton University, published paper titled Friction Factors for Pipe Flow. The work of Moody, and the Moody Diagram has become the basis for many of the calculations on friction loss in pipes and ductwork.

[6]Table for Relative roughness for some common materials was taken from website http://www.engineeringtoolbox.com.

Reynolds number (R_e)	Nature of flow	Friction coefficient (λ)
< 2300	Laminar Flow	$\lambda = 64/R_e$
$2300 - 4000$	Transient Flow	Can not be determined
> 4000	Turbulent Flow	$\frac{1}{\sqrt{\lambda}} = -2.0 log_{10}\left[2.51/\left(R_e\sqrt{\lambda}\right) + r_p/3.72d_h\right]$

Table 2: Reynolds Number, Nature of Flow and Friction coefficient (λ).

this more clearly.

We can summarize above discussion in these points

- If the Reynolds numbers is less than about 2100 the flow will be laminar. This indicates that the viscous force of the fluid is dominating the other forces that may disturb the flow. When flow is laminar, the fluid seems to move in controlled manner with regular streamlines. It would look like very thin glass films are sliding over each other.

- If the Reynolds number is between 2300 and 3000 the flow will be transient. This is category between laminar and turbulent flow, where we can not determine anything about the flow. There may also be observed a small amount of turbulence in the flow.

- If the Reynolds number is greater than 3000 which is common when the fluid is moving with high speed or with some obstacles or rough surface of duct then the flow is said to be turbulent. The flow being turbulent indicates that the inertial forces are more than forces due to velocity and that the streamlines are no more parallel to each other and the flow pattern is irregular and the fluid particles may cross one point in domain more than once.

4.3 Minor head loss

Minor losses (losses due to various attachments and change in momentum) can be calculated by following formula.

$$p_{major} = H_L\left(\frac{v^2}{2g}\right)$$

Where, H_L is loss coefficient for the pipe component and g is acceleration due to gravity.

The loss coefficients for various pipe components are available in several textbooks, man-

uals and supplier manuals. Table-3[7] lists minor loss coefficients for some common components in pipe networks. These relative roughness for materials were determined by experiments.

Type of Component or Fitting	Minor Loss Coefficient (H_L)
Flanged Tees, Line Flow	0.2
Threaded Tees, Line Flow	0.9
Flanged Tees, Branched Flow	1.0
Threaded Tees, Branch Flow	2.0
Flanged Regular 90° Elbows	0.3
Threaded Regular 90° Elbows	1.5
Threaded Regular 90° Elbows	0.4
Flanged Long Radius 90° Elbows	0.2
Threaded Long Radius 90° Elbows	0.7
Flanged Long Radius 90° Elbows	0.2
Flanged 180° Return Bends	0.2
Threaded 180° Return Bends	1.5
Fully Open Globe Valve	10
Fully Open Angle Valve	2

Table 3: Minor loss coefficients for some of the most common used components in pipe and tube systems

As mentioned before several textbooks, manuals and supplier manuals. Values in various sources may vary depending upon the experimental conditions, formulas and calculation techniques used. Thus, one must first determine if the experimental conditions of the data are the same as the conditions of the current experiment and the other additional data related to the same experiment are from the source.

4.4   Using the Moody Diagram

Head loss is a function of Reynolds number and relative roughness coefficient. Colebrook developed an empirical transition[8] function for commercial pipes, which relates friction factor and the Reynolds number. The Moody diagram is based on the Colebrook equation in the turbulent regime. The Moody chart relates the friction factor for fully developed pipe flow to the Reynolds number and relative roughness of a circular pipe. The frictional factor (λ) for head loss can be determined if Reynolds number and the relative roughness of the pipe are known. The rougher the pipe the more turbulent the flow is through that

---

[7]Table for Minor loss coefficients was taken from website http://www.engineeringtoolbox.com.

[8]'Transition' is the term used by Colebrook to describe roughness of pipe. By 'transition' he meant that the pipes are neither too rough nor too smooth.

pipe. The relative roughness of a pipe is given by e/D, where e is absolute roughness of pipe and D is diameter of pipe.
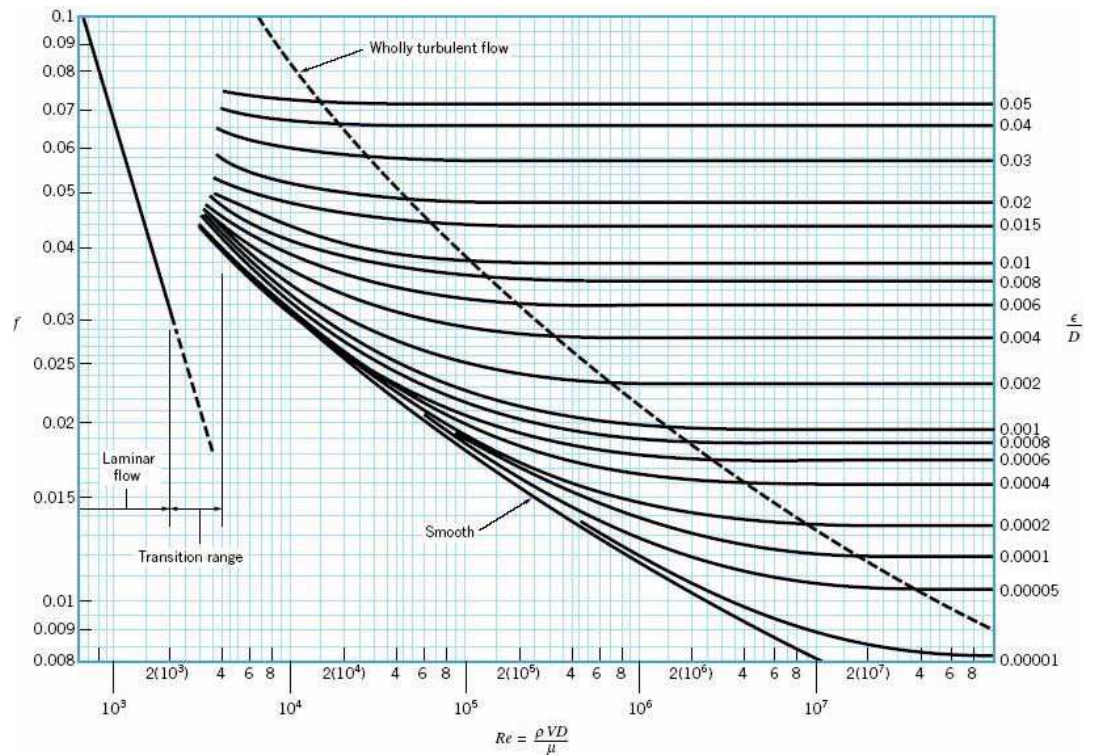
Figure 4.2: Moody chart for estimating Frictional factor

By looking at the Moody diagram it shows that the right top corner is completely turbulent and the left top is laminar (smooth flow). To determine the frictional factor, find the relative roughness value for the pipe on the right. Then locate the pipes Reynolds number on the bottom. Follow the relative roughness curve to where it crosses the determined Reynolds number. Now at that point project a straight line to the left, the number determined on the left is the frictional factor.

4.4.1 Example of using Moody chart

Consider flow situation where pipe diameter (D) is $1\ ft$, Kinematic Viscosity is $14.1 \times 10^{-6}\ \frac{ft^2}{s}$, velocity of fluid is $0.141\ \frac{ft}{s}$ and e is $0.002\ ft$.

First we compute e/D and R.

$$\frac{e}{D} = \frac{0.002\,ft}{1\,ft} = 0.002$$

$$R = \frac{Dv}{\varsigma} = \frac{(1\,ft)(0.141\frac{ft}{s})}{14.1 \times 10^{-6}\frac{ft^2}{s}} = 10000$$

Now, we consider the value of e/D and follow the curve where R is 10000. We project a straight line to left and can see that the value is 0.034.

4.5   Total Head Loss in Serial Connected Pipes

If total head loss in a single pipe is given by

$$\lambda\frac{L}{D}\frac{V^2}{2g} + K_L\frac{V^2}{2g} \tag{4.2}$$

Then, the total head loss in several serial connected pipes is algebraic sum of all the head losses due to pipes in the network. In network of k pipes, if i is the number of pipe the the total head loss can be expressed as the following formula:

$$h = \sum_{k}^{i=1}\left(\lambda_i\frac{L_i}{D_i}\frac{V_i^2}{2g} + K_{L_i}\frac{V_i^2}{2g}\right) \tag{4.3}$$

Where, the quantities with index i is connected to i^{th} pipe in the network.

5 Head Loss Coefficient for T-junction

The pressure loss caused by the T-junction depends on inner radius of the branches, velocity of fluid entering or leaving from the junction and the angle of the junction (there are various approaches for this calculations, some cases are presented in the following text). There are some classical formulas for pressure loss co-efficient for T-junctions. Most of these formulas depending on angle of T-junction, inlet and outlet velocities. To compute head loss coefficients, we have used formulas derived by A. Vazsonyi[9], A. Gardel[10] and V. Curic[11].

One other idea for computing pressure loss co-efficient for T-junctions with angles, was to consider T-junction as combination of two pipe components e.g two elbows or an elbow and a contraction. According to this idea, we assume the T-junction to be made up of two pipe components. The choice of components would depend on the flow conditions i.e from which arms the flow is coming toward the junction and from which arms the flow is leaving from the junction.

In this section we shall mention the classical formulas and the formulas that were constructed by assuming T-junction to be made up of other pipe components.

5.1 For dividing flows

These formulas are used for the situation where flow from a single branch flows to the other two remaining branches. The picture in the left of figure (5.1) gives more clear idea about such flow situations.

Various studies have been made on T-junction with dividing flow situation. Of these studies, results obtained by Andrew Vazsonyi's were believed to be the closest to the available statistical data then. Vazsonyi derived two formulas for dividing case and combining cases (5.1). In his work he explained relation between velocity ratios, angles of the junction and loss coefficient. The formulas are the result of the comparisons made by him.

---

[9] The reference book [2] contains 'Vazsonyi, Andrew: Pressure Loss in Elbows and Duct Branches. Trans. ASME, vol. 66, no. 3, Apr. 1944, pp. 177-183' as one of the important reference for these formula.

[10] The reference book [1] contains 'A. Gardel, Pressure drops in flows through T-shaped pipe-fittings, Bull. Tech. Suisse Romande 9 (1957), pp. 122130' as one of the important reference for these formula.

[11] Full derivations and details of the formulas derived by considering T-junction as two components are available in [3]

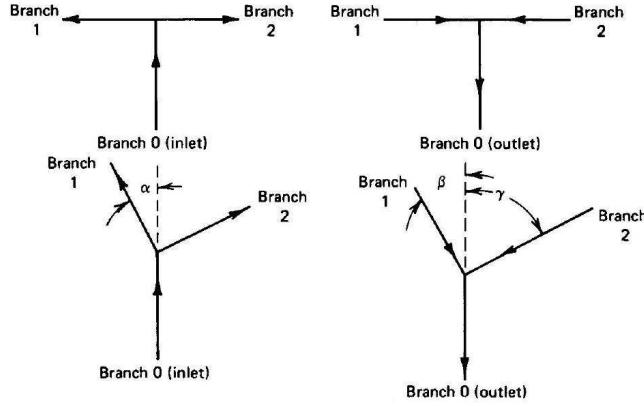The formula available from work of Vazsonyi is as following

Figure 5.1: Example of flow situations and angles for combining and dividing flow

$$K_{0,1} = \lambda_1 + (2\lambda_2 - \lambda_1)\left(\frac{V_1}{V_0}\right)^2 - 2\lambda_2\left(\frac{V_1}{V_0}\right)\cos\alpha' \qquad (5.1)$$

Here K is depending on kinetic energy of the combined flow in branch-0, and

$$\lambda_1 = 0.0712\alpha^{0.7141} + 0.37 \ \ for \ \alpha < 22.5^0 \qquad (5.2)$$

$$\lambda_1 = 1.0 \ \ for \ \alpha \geq 22.5^0 \qquad (5.3)$$

$$\lambda_2 = 0.0592\alpha^{0.7029} + 0.37 \ \ for \ \alpha < 22.5^0 \qquad (5.4)$$

$$\lambda_3 = 0.9 \ \ for \ \alpha \geq 22.5^0 \qquad (5.5)$$

and

$$\alpha' = 1.41\alpha - 0.00594\alpha^2 \qquad (5.6)$$

The figure (5.1) shows the plots for λ_1, λ_2 (left) and plot for λ_3 (right).

The other empirical formula obtained by Gardel (1957). His idea was to calculate pressure loss coefficients separately for each inlet (loss coefficient for flow from inlet-1 to outlet-3 and loss coefficient for flow from inlet-2 to outlet-3), so for each flow situation we have two loss coefficients (K_{31} and K_{32}). These formulas were derived by applying momentum balance to the main pipe section of the junction (section $abcd$ in fig (5.3)) and equation of continuity to the whole t-junction. Then energy balance is applied individually for each inlet.
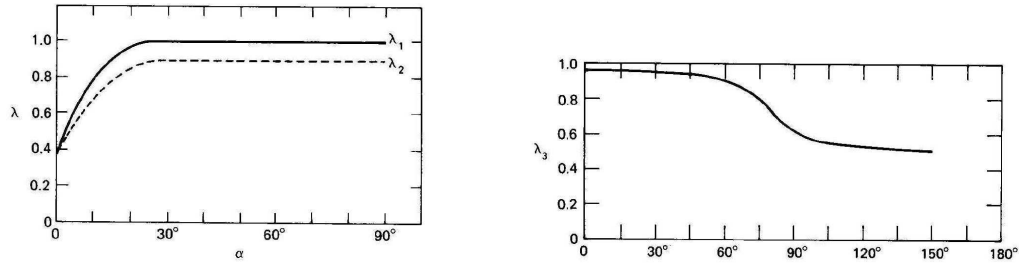
31

Figure 5.2: Plot of λ_3 (left) and Plot of α and β (right)
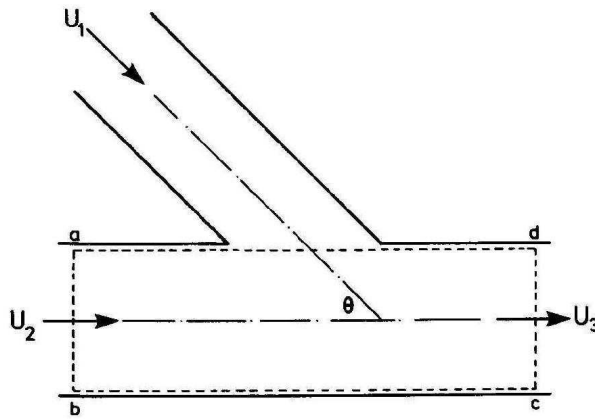

Figure 5.3: Diagram for combining flow

The formula obtained by Gardel are,

$$
K_{31} = 0.95 \left(1 - q\right)^2 + q^2 \left[\left(1.3 \tan \frac{\phi}{2} - 0.3 + \frac{0.4 - 0.1a}{a^2}\right) \left(1 - 0.9 \left(\frac{r}{a}\right)^{\frac{1}{2}}\right) \right] \\
+ 0.4q \left(\frac{1 + a}{a} \tan \frac{\phi}{2}\right) \tag{5.7}
$$

$$
K_{32} = 0.03(1 - q)^2 + 0.35q^2 - 0.2q(1 - q) \tag{5.8}
$$

Where, $a = A_1/A_3$ and $\phi = \pi - \theta$.

It can be clearly observed that there is no effect of area ratio or radius of pipe on the loss coefficient K_{32}.

5.2 For combining flows

These formulas are used for the situation where flow from two branches combine in the remaining branch. The figure (5.3) gives more clear idea about such flow situations. The formula available from work of Vazsonyi are as follows

$$K_{0,1} = \lambda_3 \left(\frac{V_1}{V_0} \right)^2 + 1 - 2 \left[\left(\frac{V_1}{V_0} \right) \left(\frac{Q_1}{Q_0} \right) \cos \beta' + \left(\frac{V_2}{V_0} \right) \left(\frac{Q_2}{Q_0} \right) \cos \alpha' \right] \tag{5.9}$$

Where, K is again depending on kinetic energy of the combined flow in branch-0. Q is volumetric flow rate ($= AV$). λ_3 is defined in the graph given by figure (5.1) and α', β' are calculated as similar to equation (5.4).

It was also stated by Vazsonyi that there is no variation of the loss coefficient with Reynolds number ($R_D > 1000$).

The other empirical formula obtained by Gardel (1957) are given by

$$K_{31} = -0.92(1-q)^2 - q^2 \left(1.2 - r^{\frac{1}{2}} \right) \left(\frac{\cos \theta}{a} - 1 \right) + 0.8q^2 \left(1 - \frac{1}{a^2} \right)$$
$$-0.8q^2 \left(\frac{1}{a} - 1 \right) \cos \theta + (2-a)(1-q)q \tag{5.10}$$

$$K_{23} = 0.03(1-q)^2 - q^2 \left[1 + \left(1.62 - r^{\frac{1}{2}} \right) \left(\frac{\cos \theta}{a} - 1 \right) - 0.38(1-a) \right] + (2-a)(1-q)q \tag{5.11}$$

Where, $a = A_1/A_3$

5.3 Combined Formula

For certain flow conditions we can assume the T-junction to be made up of other pipe components like elbows, sudden contraction or sudden expansion. To calculate pressure loss of such combination we consider pressure loss caused by the components individually and then add them. The following figures and formulas can explain this very easily. This idea was used by Vladimir Curic in his work [3]. The full details of the derivation of these formulas are available in his work. The formulas in this section were taken from his work.

T-junction as combination of an elbow and a contraction

For a combining flow situation as described in figure (5.3), T-junction can be considered as combination of an elbow and a contraction. For computing the pressure loss for such combination, we can compute pressure loss for the components separately and then add them. For doing so, we have to find the point where the elbow and contraction are joined. For this purpose, we need to solve equation (5.16) for x. The loss coefficient for elbow is
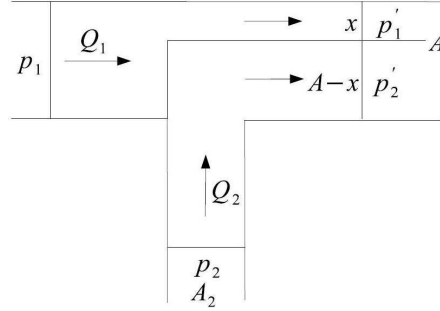

Figure 5.4: T-junction as combination of an elbow and a contraction

$$K_{23} = 0.61 \left(\frac{V_2}{V_3} \right)^2 + 1 - 2 \left(\frac{V_2}{V_3} \right) \left(\frac{Q_2}{Q_3} \right) \cos \alpha' \qquad (5.12)$$

Where $V_2 = Q_2/A_2$ and $V_3 = Q_3/(A - x)$.

And, loss coefficient for sudden contraction is

$$K_{13} = 1 - \frac{x}{A} \qquad (5.13)$$

These values can be substituted in the following formulas to determine the pressure loss.

$$p_1 - \acute{p_1} = \frac{1}{2} \rho K_{13} \left(\frac{Q_1}{x} \right)^2 \qquad (5.14)$$

and

$$p_2 - \acute{p_2} = \frac{1}{2} \rho K_{23} \left(\frac{Q_2}{A - x} \right)^2 \qquad (5.15)$$

The unknown x can be determine by solving the equation

$$p_1 - p_2 = \frac{1}{2} \rho \left\{ \left(\frac{A - x}{A} \right) \left(\frac{Q_1}{x} \right)^2 - \left(\left(\frac{0.61}{A_2^2} \right) + \left(\frac{1}{(A - x)^2} \right) \right) Q_2 + 2 \cos \alpha' \left(\frac{Q_2^2}{A_2(A - x)} \right) \right\}$$
$$(5.16)$$

34

T-junction as combination of two elbows

For a combining flow situation as described in figure (5.5), T-junction can be considered as combination of two elbows. For computing the pressure loss for such combination, we can compute pressure loss for the elbows separately and then add them. For doing so, we have to find the point where the two elbow are joined. For this purpose, we need to solve equation (5.21) for x.
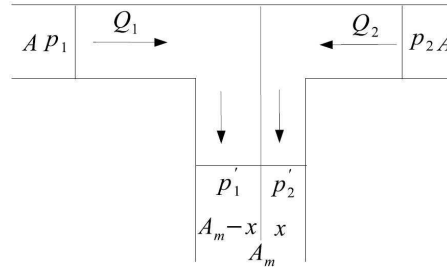

Figure 5.5: T-junction as combination of two elbows

For elbow-1, the loss coefficient is

$$K_{13} = 0.61 \left(\frac{A_m - x}{A} \right)^2 + 1 - 2 \left(\frac{A_m - x}{A} \right) \cos \alpha' \tag{5.17}$$

For elbow-2, the loss coefficient is

$$K_{23} = 0.61 \left(\frac{x}{A} \right)^2 + 1 - 2 \left(\frac{x}{A} \right) \cos \beta' \tag{5.18}$$

These values can be substituted in the following formulas to determine the pressure loss.

$$p_1 - \acute{p_1} = \frac{1}{2}\rho K_{13} \left(\frac{Q_1}{A_m - x} \right)^2 \tag{5.19}$$

and

$$p_2 - \acute{p_2} = \frac{1}{2}\rho K_{23} \left(\frac{Q_2}{x} \right)^2 \tag{5.20}$$

The unknown x can be determine by solving the equation

$$p_1 - p_2 = \frac{1}{2}\rho \left\{ 0.61 \left(\frac{Q_1^2 - Q_2^2}{A^2} \right) + \frac{Q_1}{A_m - x}^2 - \frac{Q_2}{x}^2 - 2\frac{Q_1^2}{A(A_m - x)} \cos \alpha' - 2\frac{Q_2^2}{A.x} \cos \beta' \right\} \tag{5.21}$$

6 Computational Experiments

In this section we shall discuss observations and results obtained by experiments made with softwares FLUENT and Comsol Multiphysics. We shall also compare the results obtained by softwares with the results obtained from various classical head loss formulas mentioned in last chapter. The section includes results obtained by experiments with
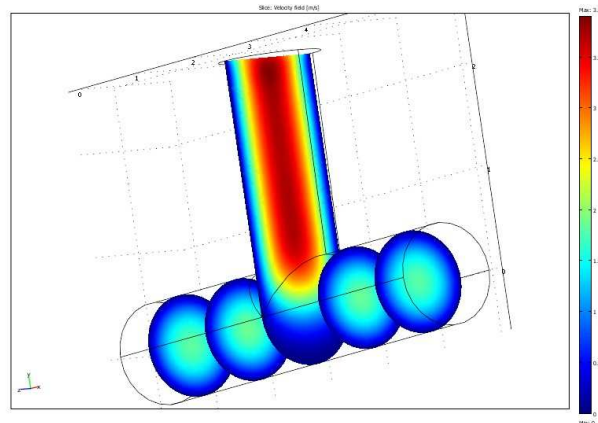

Figure 6.1: Cross-section plot for example case of flow in T-junction

T-junction with various diameters and inflow velocities, numerical results obtained by slightly changing the angle of the junction from 90^0 and also, we shall also explain how the T-junction can be split in to two pipe components (e.g. two elbows) and compare the head loss obtained by classical formula of the head loss of T-junction and formula obtained by splitting T-junction in to two pipe components.

Figure 6.2 shows and example of comparison of head-loss by classical formula and head loss observed by software of an example cases of flow in T-junction. The curve with data points presented by star is the curve for head loss observed by software and the curve with data points presented by square is the curve for head-loss obtained by classical formula. We can clearly observe that the curves agree good for first 3 sets of velocities but then on the curves do not agree.

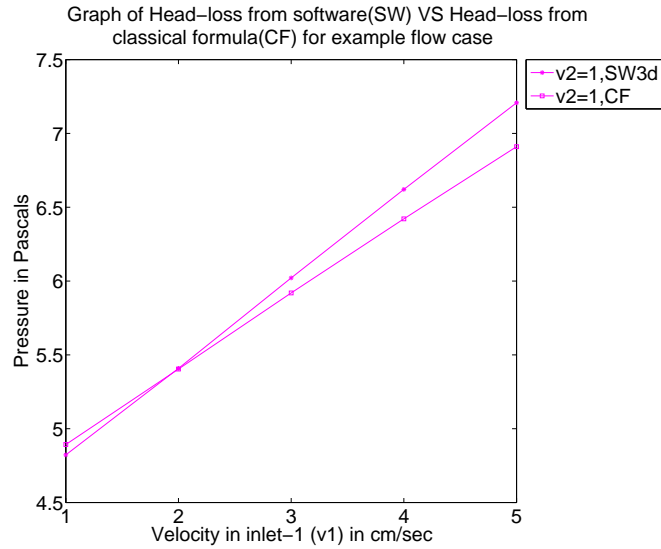The graphs in the following section can be similarly interpreted.

Figure 6.2: Comparison of head-loss by classical formula and head loss by software of an example cases of flow in T-junction

6.1 Head loss comparison for combining flow

Case-1 This is the case where the flow in coming toward the junction from two branches in main pipe and leaving from the junction from the perpendicular branch (See figure 6.3).
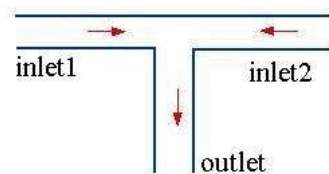

Figure 6.3: Combining flow: Case-1

From figure 6.4, it can be observed that the head loss by software and classical formulas (using the formula by Andrew Vazsonyi) do not agree in this case. There is about 3.2 % error between results by software and classical formula.

Case-2 This is the case where the flow in coming toward the junction from one branch
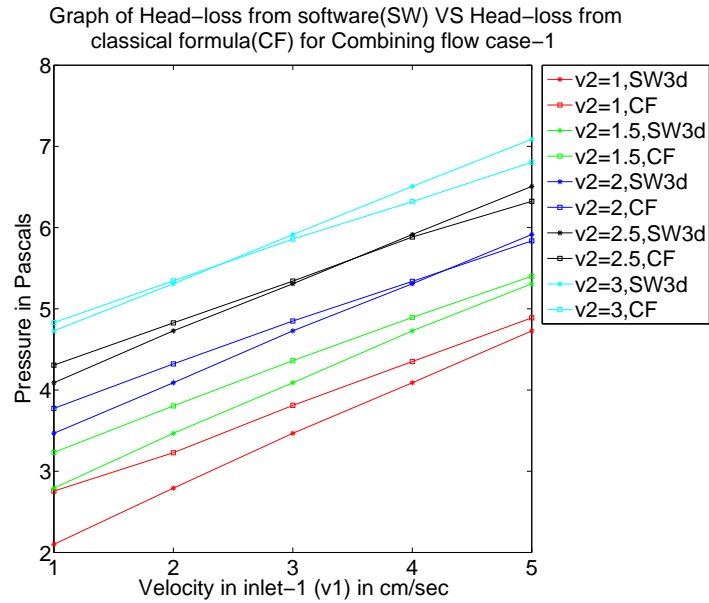
Figure 6.4: Head loss for Combining flow: Case-1, Radius of branches is 0.5 cms, Inlet velocities vary from $1\ cm/sec$ to $3\ cm/sec$ (25 different cases plotted), Outlet pressure is 100 Pascals and classical pressure loss formula by Andrew Vazsonyi

in main pipe and the branch perpendicular to it and leaving from the junction from the remaining branch in the main pipe (See figure 6.5) [The other situation is exactly the mirror image].
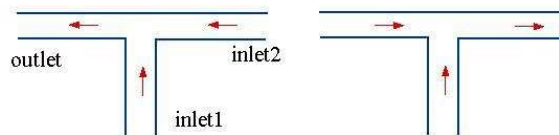

Figure 6.5: Combining flow: Cases-2

From figure 6.6, we can observe that the head loss by software and classical formulas also do not agree in this case. There is about 5.0 % error between results by software and classical formula.

38
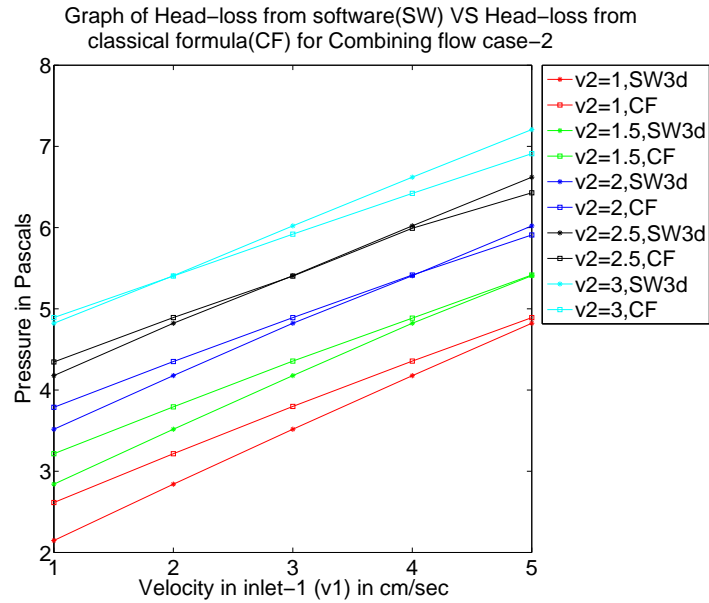
Figure 6.6: Head loss for Combining flow: Case-2, Radius of branches is 0.5 cms, Inlet velocities vary from $1\,cm/sec$ to $3\,cm/sec$ (25 different cases plotted), Outlet pressure is 100 Pascals and Classical pressure loss formula by A. Gardel

6.2 Head loss comparison for dividing flow

Case-1 This is the case where the flow in coming toward the junction from the perpendicular branch and leaving from the junction from two branches in main pipe (See figure 6.7).

Figure 6.7: Dividing flow: Case-1

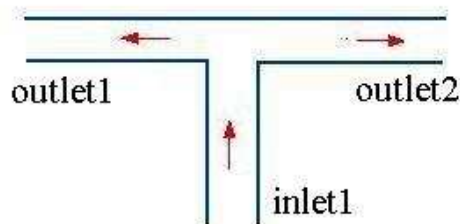**Case-2** This is the case where the flow in coming toward the junction from one branch
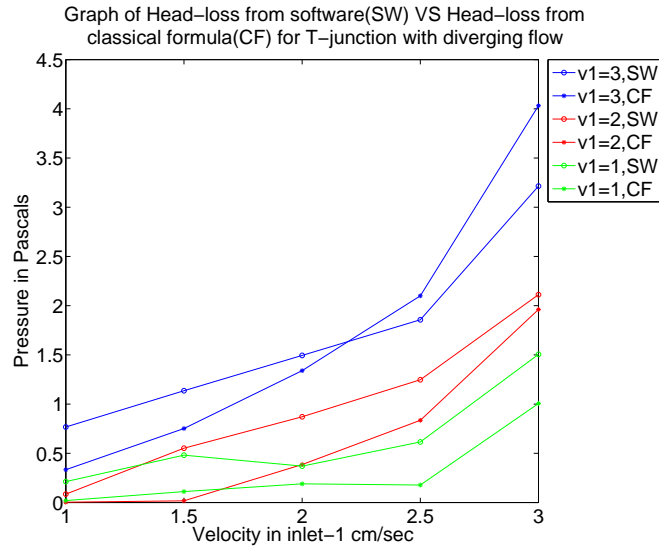
Figure 6.8: Head loss for dividing flow: Case-1, Radius of branches is 0.5 cms, Inlet velocity vary from 1 cm/sec to 3 cm/sec, at both outlet pressure is 100 Pascals and Classical pressure loss formula by A. Gardel

in main pipe and perpendicular branch and leaving from the junction from the remaining branch in the main pipe (See figure 6.9) [The other situation is exactly the mirror image]
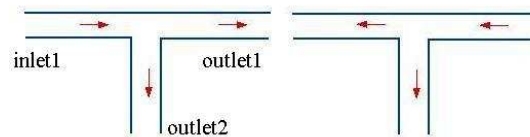
Figure 6.9: Dividing flow: Case-2

From figure 6.8 and 6.8, we can observe that the head loss by software and classical formulas also do not agree in this case. Though the curves, seem to get along with the increase in inlet velocities, but they do not exactly match for any combination of velocities. There is about 4.5 to 6.1 % error between results by software and classical formula.

6.3 Head loss change with change in angle of T-junction branches

In this part we shall display comparison of head loss obtained by software and classical formulas for different angles of T-junction. The figure 6.11 cases for inflow, outflow and
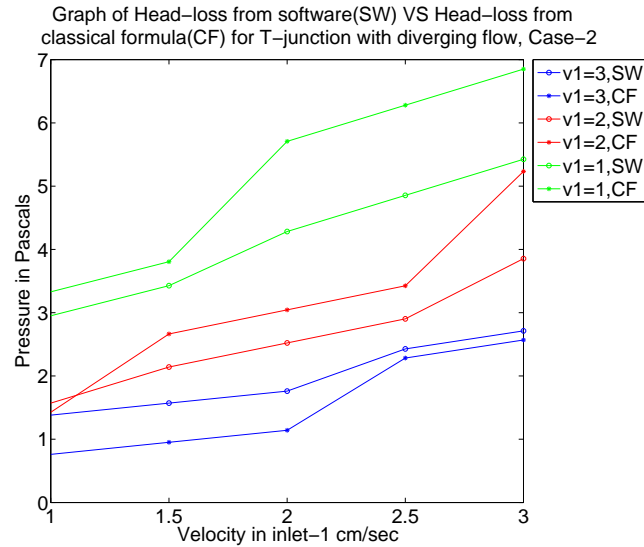
Figure 6.10: Head loss for dividing flow: Case-2, Radius of branches is 0.5 cms, Inlet velocity vary from $1\ cm/sec$ to $3\ cm/sec$, at both outlet pressure is 100 Pascals and Classical pressure loss formula by A. Gardel

angle. For all the comparisons we have use formulas by Andrew Vazsonyi for combining flow case-1 and formulas by A. Gardel for case-2.
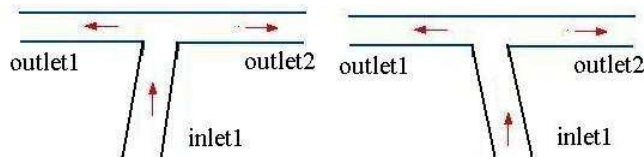
Figure 6.11: T-junction with different angles between main pipe and branch pipe

In cases shown in figure-6.12 to figure-6.17, we have calculated and compared head loss suffered by T-junction with angle $\gamma = 91$, $\gamma = 91$, $\gamma = 93$, $\gamma = 89$, $\gamma = 88$ and $\gamma = 87$. These calculations were for combining flow case-1, where flow is coming toward the junction from opposite pipes and leaving from the junction through perpendicular pipe (see figure 6.3). It was observed that the head loss increases with increase in angle. Also, for all the cases; the head loss obtained by software and classical formula were close to each other.

Figure 6.12: Head loss for T-junction with angle $\gamma = 91$, combining flow: Case-1, Radius of branches is 0.5 cms, Inlet velocities vary from $1\,cm/sec$ to $3\,cm/sec$ (25 different cases plotted), Outlet pressure is 100 Pascals and Classical pressure loss formula by Andrew Vazsonyi

The figure 6.18 shows head loss for different angles of T-junction. These calculations were for combining flow case-2, where flow is coming toward the junction from perpendicular pipes and leaving from the j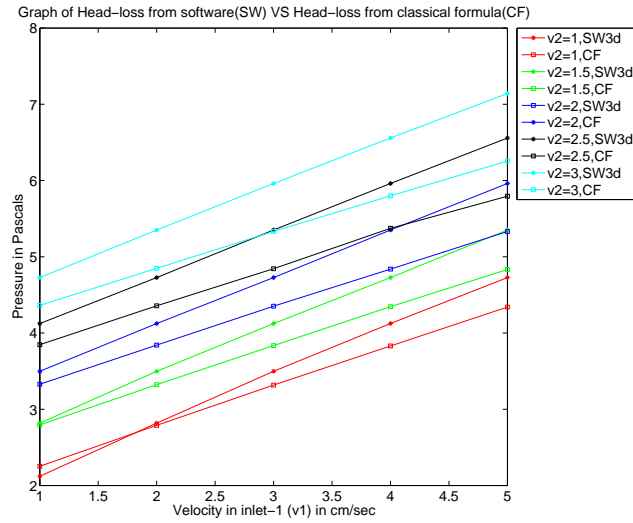unction through remaining main pipe (see figure 6.5). It was observed that when the angle gamma (γ) is less, head loss suffered is less. This is because there is no significant change in of momentum of the flow between incoming and out going flow. It was also observed that when the angle gamma (γ) is more, head loss suffered is more. This is because of change in momentum of the flow while passing through T-junction.

From the cases $\gamma = 87$ (fig-6.15), $\gamma = 88$ (fig-6.16), $\gamma = 89$ (fig-6.17), $\gamma = 91$ (fig-6.12), $\gamma = 92$ (fig-6.13) and $\gamma = 93$ (fig-6.14), we can observe that the head loss by software and classical formulas also do not agree in any case. Though for some cases and certain inlet velocity combinations, the curves seem to get along with each other but this is not sufficient to conclude that the head losses obtained by both the sources agree. There is about 4.6 to 6.7 % error between results by software and classical formula.
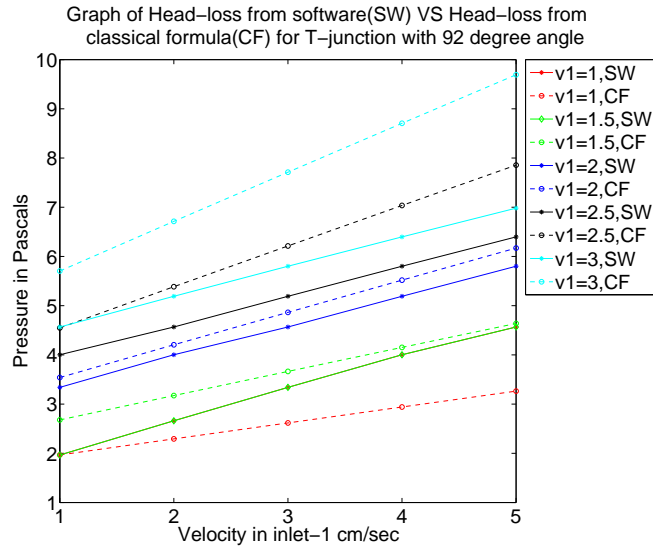
Figure 6.13: Head loss for T-junction with angle $\gamma = 92$, combining flow: Case-1, Radius of branches is 0.5 cms, Inlet velocities vary from $1\,cm/sec$ to $3\,cm/sec$ (25 different cases plotted), Outlet pressure is 100 Pascals and Classical pressure loss formula by Andrew Vazsonyi

6.4 Head loss for T-junction with different radius of branches

Case-1: This is the case where the cross-section area of main pipe is one half of that of perpendicular branch pipe. The flow is coming toward the junction from the opposite branches in main pipe and leaving from the perpendicular branch (See figure 6.19).

Case-2: This is the case where the cross-section area of main pipe is one third of perpendicular branch pipe. The flow is coming toward the junction from the opposite branches in main pipe and leaving from the perpendicular branch (See figure 6.21).

Case-3: This is the case where the cross-section area of main pipe is one fourth of perpendicular branch pipe. The flow is coming toward the junction from the opposite branches in main pipe and leaving from the perpendicular branch similar to above two cases.

The figure 6.24 shows head loss for different cross-section areas of branches of T-junction ($A1 =$area of main pipe, $A2 =$area of branch pipe). These calculations were for combining flow case-1, where flow is coming toward the junction from opposite branches in main pipe and leaving the junction from perpendicular branch pipes (see figure 6.5).

From figure 6.20, figure 6.22 and figure 6.23 we can observe that the head loss by software
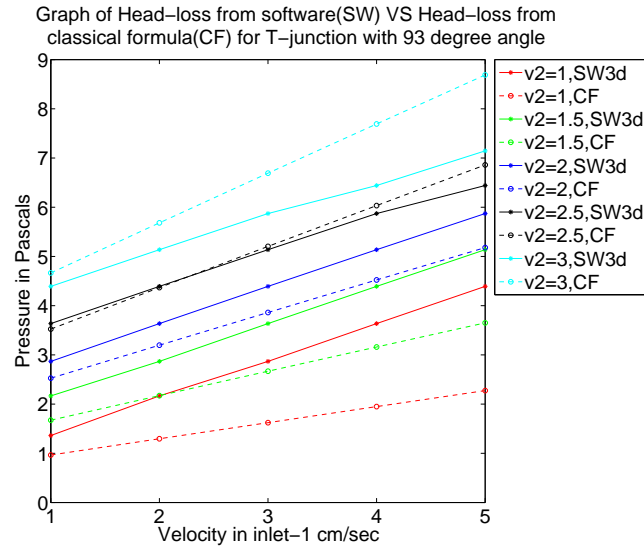
43

Figure 6.14: Head loss for T-junction with angle $\gamma = 93$, combining flow: Case-1, Radius of branches is 0.5 cms, Inlet velocities vary from $1\ cm/sec$ to $3\ cm/sec$ (25 different cases plotted), Outlet pressure is 100 Pascals and Classical pressure loss formula by Andrew Vazsonyi

and classical formulas also do not agree. There is about 4.4 to 6.8 % error between results by software and classical formula.

It was observed that head loss is reducing when the cross-section area of the main pipe is reducing (for all the cases cross-section area of the perpendicular branch pipe was kept same 1 cm.). This observations also verifies claims by A. Gardel, that the head loss increases with increase in ratio of the cross section area ($A2/A1$ where, $A1$ =area of main pipe, $A2$ =area of branch pipe). These observations are for the case when the flow is combining case-1, where the flow is coming in from opposite branches in main pipe and leaving from perpendicular branch pipe. The observation is exactly reverse when we consider combining flow case-2, where the flow is coming in from one branch in main pipe and perpendicular branch pipe and leaving from remaining branch in main pipe. The head loss suffered will increase with increase in ratio of the cross section area ($A2/A1$).

Figure 6.15: Head loss for T-junction with angle $\gamma = 87$, combining flow: Case-1, Radius of branches is 0.5 cms, Inlet velocities vary from $1\,cm/sec$ to $3\,cm/sec$ (25 different cases plotted), Outlet pressure is 100 Pascals and Classical pressure loss formula by Andrew Vazsonyi

Figure 6.16: Head loss for T-junction with angle $\gamma = 88$, combining flow: Case-1, Radius of branches is 0.5 cms, Inlet velocities vary from $1\,cm/sec$ to $3\,cm/sec$ (25 different cases plotted), Outlet pressure is 100 Pascals and Classical pressure loss formula by Andrew Vazsonyi
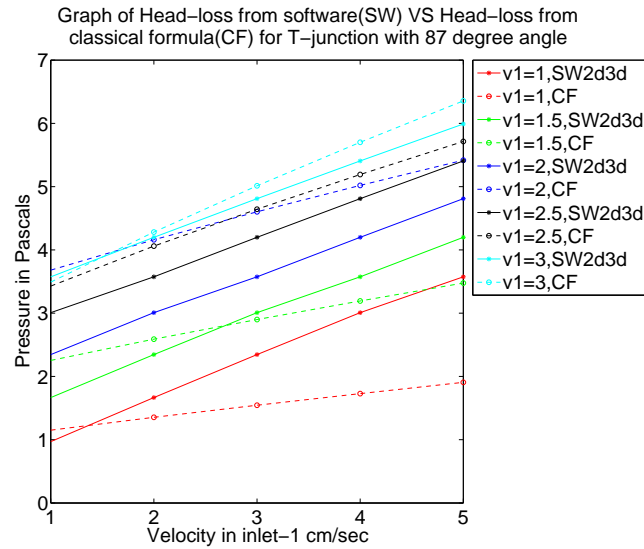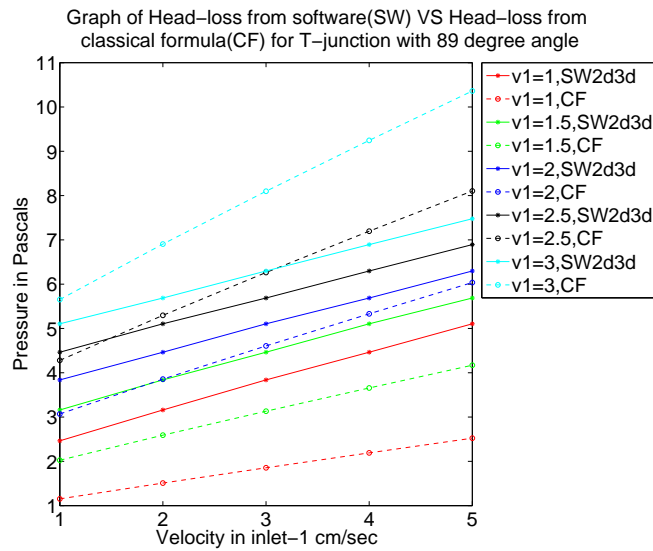
Figure 6.17: Head loss for T-junction with angle $\gamma = 89$, combining flow: Case-1, Radius of branches is 0.5 cms, Inlet velocities vary from $1\ cm/sec$ to $3\ cm/sec$ (25 different cases plotted), Outlet pressure is 100 Pascals and Classical pressure loss formula by Andrew Vazsonyi

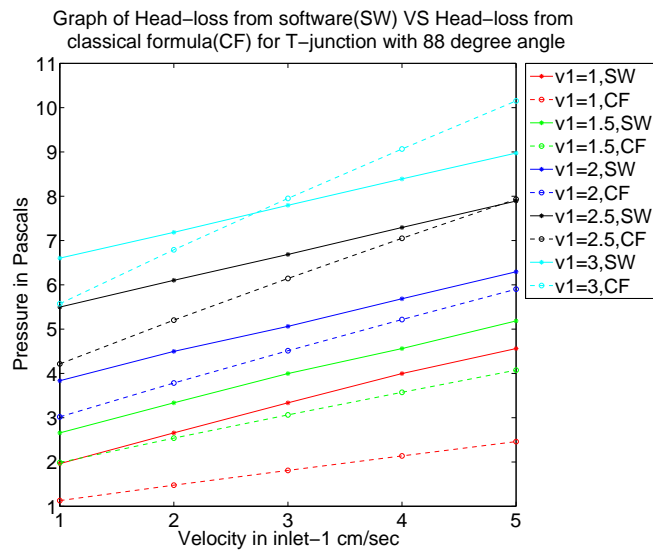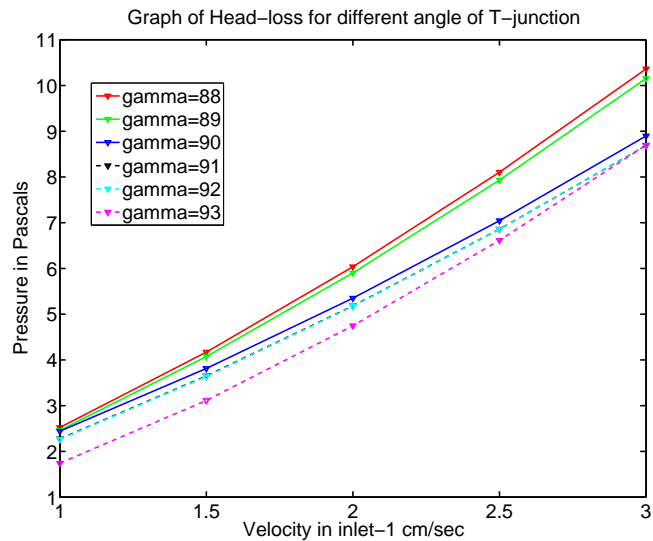Figure 6.18: Head loss for different angle of T-junction, combining flow: Case-2, Radius of branches is 0.5 cms, Inlet velocities vary from $1\ cm/sec$ to $3\ cm/sec$, Outlet pressure is 100 Pascals and Classical pressure loss formula by A. Gardel
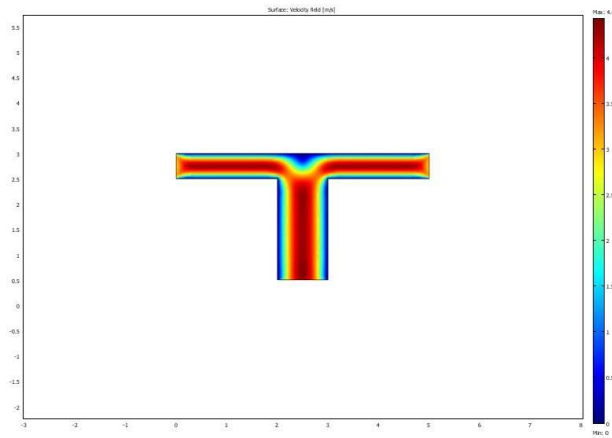
Figure 6.19: Dividing flow: Case-1
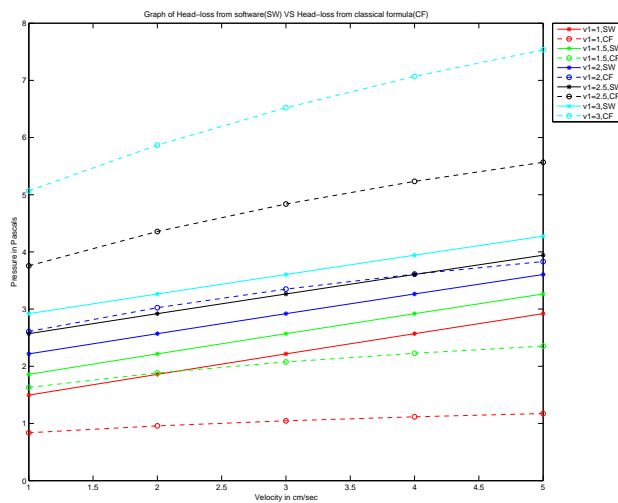
Figure 6.20: Head loss for area case-1, combining flow case-1, Radius of main pipe is branches is 0.25 cms, Radius of perpendicular pipe is branches is 1 cms, Inlet velocity in both inlets vary from $1\,cm/sec$ to $3\,cm/sec$, pressure at outlet is 100 Pascals and Classical pressure loss formula by Andrew Vazsonyi

47
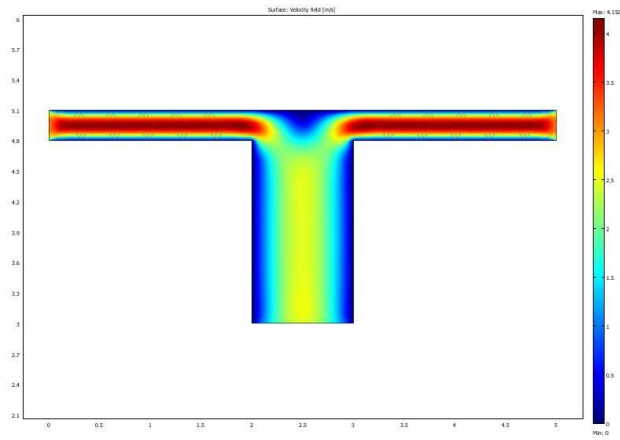
Figure 6.21: Dividing flow: Case-1
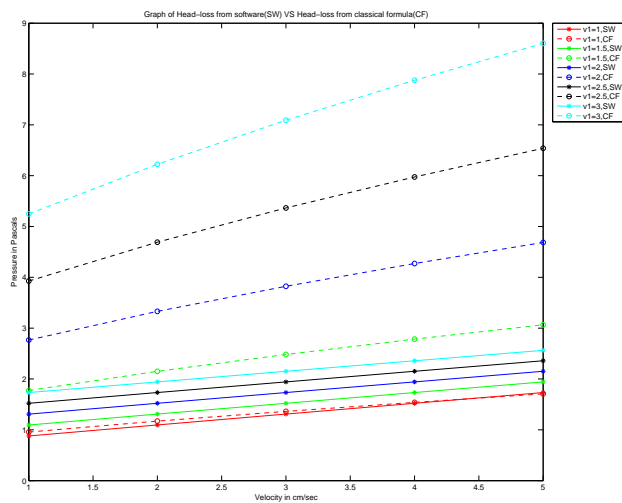
Figure 6.22: Head loss for area case-2, combining flow case-1, Radius of main pipe is branches is 0.3 cms, Radius of perpendicular pipe is branches is 1 cms, Inlet velocity in both inlets vary from $1\ cm/sec$ to $3\ cm/sec$, pressure at outlet is 100 Pascals and Classical pressure loss formula by Andrew Vazsonyi
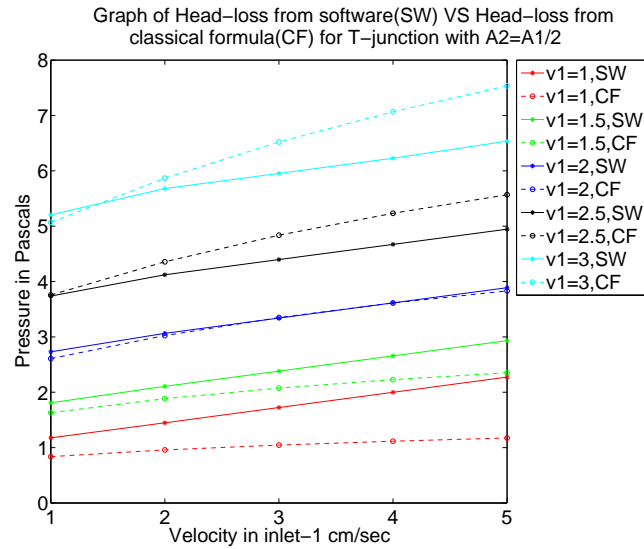
Figure 6.23: Head loss for area case-1, combining flow case-1, Radius of main pipe is branches is 0.25 cms, Radius of perpendicular pipe is branches is 1 cms, Inlet velocity in both inlets vary from $1\,cm/sec$ to $3\,cm/sec$, pressure at outlet is 100 Pascals and Classical pressure loss formula by Andrew Vazsonyi

Figure 6.24: Head-loss for different cross-section areas of branches of T-junction, $A1 =$ area of main pipe, $A2 =$ area of branch pipe, combining flow: Case-1, Radius of branches is 0.5 cms, Inlet velocities vary from $1\,cm/sec$ to $3\,cm/sec$, Outlet pressure is 100 Pascals and Classical pressure loss formula by A. Gardel
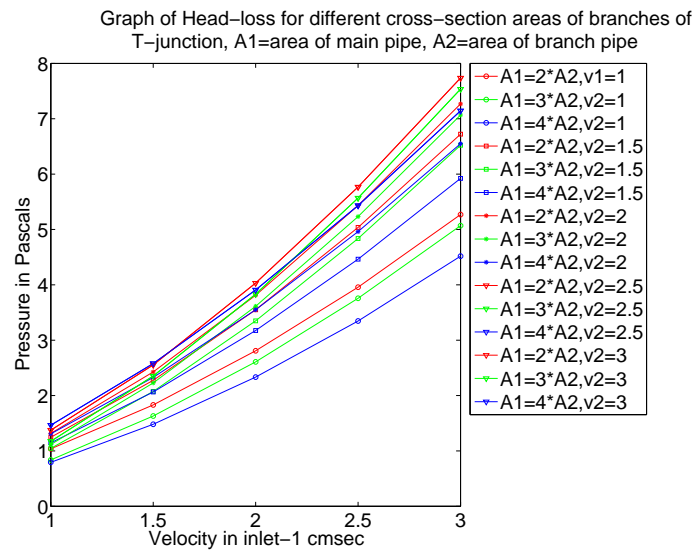
7 Discussion and future scope of the work

7.1 Discussion

From results in the previous section, we can observe that there is difference between head loss in T-junction of pipes observed by calculations from software packages Fluent and Comsol. Our main aim was to study the difference between the observations from CFD softwares and classical formula by Andrew Vazsonyi, A. Gardel and formulas available in reference [3].

In case of combining flow, the difference between observations obtained by Comsol (3D experiments) and classical formula were in the range of 3.2 to 5.1 %. Incase of dividing flow, this difference was in the range of 4.5 to 5.5 %. In the case, where we varied the angle of the T-junction from 87 degrees to 93 degrees, difference between observations by Comsol (3D experiments) and classical formula was in the range of 4.6 to 6.7 %.

One of the reasons for these errors is likely the limited capabilities of software. These differences are as a result of software's inability to handle complicated flow conditions. Comsol Multiphysics (version 3.2a) can not handle flow situations with turbulence. Also, this version of Comsol Multiphysics does not have ability to model rough inner surface of pipes.

For all our experiments the fluid was considered water with normal properties at room temperature. Also the classical formulas are valid only for fluid that is incompressible and inviscid. The formulas reference [3], with the idea of considering the T-junction as combination of two pipe components, is only valid for 2D case.

Our main aim was to study the difference between the observations from CFD software and classical formula by Andrew Vazsonyi, A. Gardel and formulas available in reference [3]. The values obtained by CFD software were in certain agreement with classical formulas both by Andrew Vazsonyi and A. Gardel but values obtained by CFD software were better agreement with A. Gardel. It can be clearly observed that for combining flow situations where we used Gardel's formula, the difference was in range of 3.2 to 5.0 % and for dividing flow cases where we used Vazsonyi formulas, the difference was in range of 4.5 to 6.0 %.

Gardel's formulas were as result of a systematic derivation from basic principles of mo-

mentum (applied to the main pipe), continuity principle to the fluid in whole T-junction and energy balance principle (individually) to flow coming from the branches. Unfortunately, none of the classical formulas consider pipe roughness as factor for the head loss. Roughness of the pipe varies from as material and it is also considered as one of the major cause for major losses. This is where the accuracy of coefficients obtained by classical formula can be questioned. Though, the loss due to friction between fluid and junction inner surface is very less, but theses small values can be very significant for precise calculations.

During this work, we also observe that the difference between observations by 2D simulations of software and classical formula were considerably larger than the difference between observations by 3D simulation of software and classical formula. We also recommend 3D simulation for such calculations, since 3D simulation are more near to the reality and also effect of turbulence can be modeled and observed in 3D simulations. Also, 3D simulation give more clear view of swirl movements, streamlines and turbulence in the fluid.

During the work we realized that Fluent is a better option for heavy and precise simulations. Since, Fluent has capability to model turbulence with verity of Kappa-Epsilon models and also because Gambit is a very handy tool to create even complicated geometries. But, Fluent can be sometimes very expensive in terms of computational time. The only advantage with Comsol Multiphysics is that we can create geometry and carry out calculations in the same environment and the grid does not have to be exported every time the experiments are repeated.

From our experience during this work, we would suggest to use Fluent for similar simulations. There are also some higher versions of Comsol available that have capability to handle complex flow situations. Gardel's formulas were as result of a systematic derivation from basic principles of momentum (applied to the main pipe[12]), continuity principle to the fluid in whole T-junction and energy balance principle (individually) to flow coming from the branches.

---

[12]For this purpose he considered main pipe as a control volume and applied momentum balance principle.

7.2   Future scope of the work

In this work was restricted to only water at room temperature and t-junctions with smooth inner surface. There can be more work done to generalize these results for the other fluids and T-junction with rough inner surfaces.

Also, with software our ambition was to construct a real time simulation of T-junction with varying angle. Though this is a very lengthy process, since fluent takes too much time with dynamic mesh, but this is possible with higher versions of fluent and other CFD packages.

Unfortunately, none of the classical formulas consider pipe roughness as factor for the head loss. Roughness of the pipe varies from as material and it is also considered as one of the major cause for major losses. This is where the accuracy of coefficients obtained by classical formula can be questioned. Though the loss due to friction between fluid and junction inner surface is very less but theses small values can be very significant for precise calculations.

During this study, we also came across an industrial problem concerning to flow of pulp like fluid in pipes. The problem was placing a valve of certain capacity for regulating supply of pulp like material based on the pressure and velocity profiles in the supply network. Initially, pipe with elastic property was used to supply the material and a large forceps was used to reduce the diameter of pipe where the supply was not needed or to be regulated. Such kind of problems can be solved with similar techniques.

In this work all, we made an attempt to study effect of different radius of main pipe and branch pipe. The range of flow parameters (flow velocity, pipe diameter and pressure) used in our computational experiments was relatively small. It is also possible that the difference of head loss observed and inaccuracy of the formula is even larger in broader range of parameters. Thus we suggest that there should be more 3D computational experiments done using more advanced CFD software packages.

This can play important role in verifying other claims made on basis of classical formulas. E.g. Andrew Gardel's observation that head-loss increases with increase in ratio of areas of main pipe and branch pipe.

References

[1] Ward-Smith A. J, *Internal fluid flow the fluid dynamics of flow in pipes and ducts,* Clarendon Press, Oxford (1980).

[2] Robert P. Benedict, *Fundamentals of Pipe Flow,* Wiley-Inter science Publications (1980).

[3] Vladimir Curic, *Matematicki model efikasnog upravljanja protokom vode,* Institute of Mathematics, University of Novi Sad, Master thesis (2007).

[4] Boris Huber, *CFD Simulation of a T-Junction,* Institute of Hydraulic and Water Resources Engineering, Department of Hydraulic Engineering, Vienna University of Technology.

[5] Ronald W. Jeppson, *Analysis of flow in pipe networks,* ANN Arbor Science (1976).

[6] Batchelor G. K, *Introduction to fluid dynamics,* Cambridge : Cambridge University Press (1990).

[7] Hozef Arif, *Application of Computational Fluid Dynamics to the modeling of horizontal wells,* Stanford University (1999).

[8] Stephen Wolfram, *Notes for Chapter 8: Implications for Everyday Systems Section: Fluid Flow-A New Kind of Science, Page 996,* www.wolframscience.com.

[9] H. Tennekes and J.L Lumley, *A First Course in Turbulence*, The MIT Press, Cambridge MA (1992).

[10] C. Foias, O. Manley, R. Rosa and R. Teman, *Navier-Stokes Equation and Turbulence,* Cambridge University Press, Cambridge (2001).

[11] Roger Temam, *Navier-Stokes equations : theory and numerical analysis,* North-Holland, Amsterdam (1984).

[12] W.D. McComb, *The Physics of Turbulence,* Oxford University Press (1990).

[13] J. M. McDonough *Introductory Lectures on Turbulence Physics: Mathematics and Modeling,* Departments of Mechanical Engineering and Mathematics, University of Kentucky (2004).

[14] Davies, Alan J, *Finite element method a first approach,*Oxford : Clarendon Press (1980).

[15] Versteeg, H. K, *Introduction to computational fluid dynamics the finite volume method,* Harlow: Longman Scientific and Technical (1995).

[16] Baker A. J, *Finite elements 1-2-3,* New York : McGraw-Hill (1991).

[17] Taylor C, *Finite element programming of the Navier-Stokes equations,* Swansea : Pineridge Press (1981).

[18] Bruce Irons and Nigel Shrive, *Finite element primer,* Glasgow : Department of Trade and Industry, National Engineering Laboratory (1986).

[19] Vivette Girault and Pierre-Arnaud Raviart, *Finite element methods for Navier-Stokes equations theory and algorithms,* Berlin: Springer, cop. (1986).

[20] O. Axelsson and V. A. Barker, *Finite element solution of boundary value problems theory and computation,* Orlando,FL : Academic Press (1984).

[21] D. W. Jordan and P. Smith, *Nonlinear ordinary differential equations,* Oxford : Clarendon Press (1983).

[22] John H. Mathews and Kurtis D. Flink, *Numerical methods using MATLAB,* Upper Saddle River (NJ) : Pearson/Prentice Hall, cop. (2004).

8 Appendix A. Elements Basis functions and Local Basis Functions

Suppose that for a given finite element mesh there is associated with each node $N_i = (x_i, y_i)$ a function ,defined on $\bar{\Omega}$ with following properties.

1. The restriction of ϕ_i to any element e_l mesh is associated with each a polynomial form

$$\phi_i(x, y) = \sum_{s=1}^{T} C^{il}_{(s)} x^{p_s} y^{q_s}$$

; $(x, y) \in e_l$ where powers p_s and q_s, $s = 1, 2, ..., T$ are independent of i and j.

2. $\phi_i(N_j) = \delta_{ij}$ for $i, j = 1, 2, ...M$

3. ϕ_i is uniquely determined on every element edge by its value at the nodes belonging to that edge.

4. $\phi_i \in C(\bar{\Omega})$

5. ϕ_i assumes non-zero values only in those elements to which N_i belongs.

6. If N_i is not on Γ,then Φ_i vanishes on the boundary of its support. If N_i in on Γ, then ϕ_i vanishes on part of boundary of its support that lies in Ω.

7. It is possible to chose a standard (or reference) element $\tilde{e}$ in the $\tilde{x} - \tilde{y}$ plane with local basis functions $\tilde{\phi}_1(\tilde{x}, \tilde{y}), ..., \tilde{\phi}_T(\tilde{x}, \tilde{y})$ of type $\phi_i(x, y) = \sum_{s=1}^{T} C^{il}_{(s)} x^{p_s} y^{q_s}$ and find for every element e_l invertible affine variable transformation.

$$x = x(\tilde{x}, \tilde{y}) = f_{11}\tilde{x} + f_{12}\tilde{y} + b_1$$

$$y = y(\tilde{x}, \tilde{y}) = f_{21}\tilde{x} + f_{22}\tilde{y} + b_2$$

$(\tilde{x}, \tilde{y}) \in \tilde{e}$ depends on l, such that this maps $\tilde{e}$ onto e_1 (mapping nodes onto nodes) and

$$\tilde{\phi}_r(\tilde{x}, \tilde{y}) = \phi^l_r(x(\tilde{x}, \tilde{y}), y(\tilde{x}, \tilde{y}))$$

denoting the inverse transformation by

$$\tilde{x} = \tilde{x}(x, y)$$

and $\tilde{y} = \tilde{y}(x, y)$ thus $(x, y) \in e_l$ We can rewrite $\tilde{\phi}_r(\tilde{x}, \tilde{y})$ as

$$\Phi_l^r(x, y) = \Phi_l^r(\tilde{x}, y)(\tilde{x}(x, y), \tilde{y}(x, y))$$

Local basis function over e_l, defined by

$$\Phi_{(l)}^r(x, y) = \Phi_{i_r(l)}^r(x, y)$$

, $(x, y) \in e_l$, $r = 1, 2, ...T$ A local basis function is simply the restriction of some global basis function to e_l.

9   Appendix B. Lax Milgram Lemma

Consider a functional

$$f(u) = \int_b^a \left\{ \frac{1}{2} p(x)(u')^2 + \frac{1}{2} q(x)(u)^2 - g(x)u \right\} dx$$

, $u \in V$

$$V = \left\{ v \in C^2[a,b]; v(a) = v(b) = 0 \right\}$$

Where, $p \in C^1[a,b]$, $q, p \in C[a,b]$, $0 < p_0 \leq p(x) \leq p_1$ and $0 < q_0 \leq q(x) \leq q_1$ for $a \leq b$ with p_0, p_1, q_1 as constants.

$$a(u,v) = \int_b^a \left\{ p(x)u'v' + q(x)uv \right\} dx$$

, $u, v \in V$

$$G(u) = \int_b^a g(x)u dx$$

, $u \in V$We can express f as, $f(u) = \frac{1}{2} a(u,u) - G(u)$, $u \in V$. Let, V be any arbitrary Hilbert Space with inner product $(.,.)_v$ and norm $\|u\|_v = (u,u)_{\frac{1}{2}}^v$; $u \in V$. Let $a : V \times V \to \Re$ be a mapping with following four properties.

1. $a(\alpha u + \beta v, w) = \alpha.a(u,w) + \beta.a(v,w)$, $u, v, w \in V$, $\alpha\beta \in \Re$

2. $a(w, \alpha u + \beta v) = \alpha.a(w,u) + \beta.a(w,v)$, $u, v, w \in V$, $\alpha\beta \in \Re$

3. $\exists$ constant $\beta \ni |a(u,v)| \leq \beta \|u\|_V \|v\|_V$, $u, v, w \in V$ i.e a is bounded.

4. $\exists$ constant $\rho > 0 \ni a(u,v) \geq \rho \|u\|_v^2$, $u \in V$ i.e a is coercive. Let $G : V \to \Re$ be a mapping with following properties :

5. $G(\alpha u + \beta v) = \alpha G(u) + \beta G(v)$; $u, v, w \in V$, $\alpha\beta \in \Re$ i.e G is linear.

6. $\exists$ constant $\delta > 0 \ni |G(u)| \leq \rho \|u\|_v$, $u \in V$ i.e G is bounded.

Under these assumptions for $'a'$ and $'a'$, there exist a unique element $\hat{u} \in V$ such that $a(\hat{u}, u) = G(u), \forall u \in V$.

10   Appendix C. Field and derivative rules

For any arbitrary fields v and w,

- $\overline{v + w} = \overline{v} + \overline{w}$

- $\overline{av} = a\overline{v}$, where a is constant.

- $\overline{a} = a$, where a is constant.

- $\overline{\dfrac{\partial v}{\partial s}} = \dfrac{\partial \overline{v}}{\partial s}$, where $s = x_i$ or $s = t$

- $\overline{\overline{v}w} = \overline{v}\overline{w}$

Some consequences of these averaging rules are as following

- $\overline{u_i u_j} = \overline{u_i}\,\overline{u_j} + \overline{u_i' u'j}$

- $\overline{u_i u_j u_k} = \overline{u_i' u_j' u_k'} + \overline{u_i' u_j'}\,\overline{u_k} + \overline{u_j' u_k'}\,\overline{ui} + \overline{u_k' u'i}\,\overline{uj} + \overline{u_i u_j u_k}$

- $\overline{\dfrac{\partial u_i}{\partial t} u_i} - \dfrac{\partial \overline{u_i}}{\partial t}\overline{u_i} = \overline{\dfrac{\partial u_j'}{\partial t} u_i'}$

Some rules for derivative

1. $\overline{\dfrac{\partial u_i}{\partial t} u_i} = \dfrac{\partial \overline{u_i}}{\partial t}\overline{u_i} + \overline{\dfrac{\partial u_i'}{\partial t} u_i'}$

2. $\overline{\dfrac{\partial p}{\partial x_i} u_i} = \dfrac{\partial \overline{p}}{\partial x_i}\overline{u_i} + \overline{\dfrac{\partial p'}{\partial u_i} u_i'}$

3. $\overline{\dfrac{\partial \tau_{ij}}{\partial x_i} u_i} = \dfrac{\partial \overline{\tau_{ij}}}{\partial x_i}\overline{u_i} + \overline{\dfrac{\partial u_i'}{\partial u_i} \tau_{ij}'}$

4. $\overline{u_j \dfrac{\partial u_i}{\partial x_j} u_i} - \overline{u_j}\dfrac{\partial \overline{u_i}}{\partial x_j}\overline{u_i} = \overline{u_i' \dfrac{\partial u_i'}{\partial x_j}}\overline{u_i} + \overline{\dfrac{\partial u_i'}{\partial x_j} u_i' u_j'} + \overline{u_i' \dfrac{\partial u_i'}{\partial x_j}}\overline{u_i} + \overline{u_i' u_i' \dfrac{\partial u_i'}{\partial x_j}}$

11   Appendix D. Creating geometry in Gambit

We can create t-junction geometry by two ways, one is creating two rectangles perpendicular to each other and then merging them second is creating vertex points and connecting them by edges. We will do this by second way.

- First we shall create the points that will be used to create the lines and then faces of the domain. **Operation > Geometry > Vertex > Create Vertex** A(0,0), B(0,5), C(5,1), D(0,1), E(2,1), F(3,1), G(2,3), H(3,3).
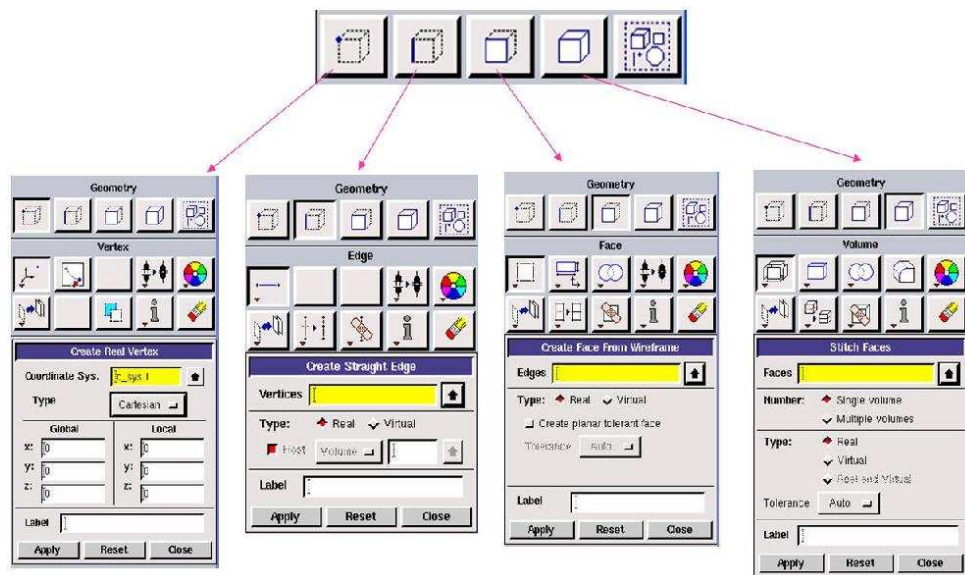

Figure 11.1: Buttons for drawing geometry

- Now draw the straight lines that will complete the domain. Connect the points to create the following line segments: AB, BC, CD, DE, EF, FG, GH, HA.

- **Operation > Geometry > Face > Form Face**. Select all the line segments in the drop list and create the face.

- **Operation > Mesh > Mesh Face**. Select the face and specify the spacing or ratio.

- **Operation > Zones > Specify Boundary Types**. Create boundary conditions as follows: Left face = **Velocity Inlet1**, Right face = **Velocity Inlet2**, Upper face = Pressure Outlet and all the other faces are **walls**.

- Save the Gambit file and **export** to the Fluent mesh.

12   Appendix D. Solving problem with fluent

- Load the mesh into Fluent. File > Read > Case.

- Check the mesh for errors. Grid > Check

- For this problem, the default Solver settings will be sufficient. Ensure that the proper viscous model is selected. **Define > Models > Viscous**.

- Now recall liquid water from the materials database so that it can be specified in the boundary conditions. **Define > Materials**. Enter the database by clicking on Database. Select water liquid (h2o<l>) in the Fluid Materials list. Click Copy and then Close. Now move the reference pressure into the flow domain.

- **Define > Operating Conditions**.

- Boundary conditions can now be set. Define > Boundary Conditions. Select fluid in the selection menu on the left and then click on Set. Change Material Name to water-liquid. Now click on inlet in the Zones menu and enter the velocity-inlet window. Change Velocity Specification Method to Components and enter a velocity of 2.01e-4 m/s (liquid water at Re = 20) next to X-Velocity. Change the discretization method to a higher order scheme.

- **Solve > Controls > Solution**. Change the Discretization for Momentum to 2nd Order Upwind.

- The flow domain can now be initialized. **Solve > Initialize > Initialize**. Initialize the flow with the inlet conditions.

- Enable the plotting option for residuals and turn off automatic convergence checking. **Solve > Monitors > Residual**.

- The problem is ready to be iterated. **Solve > Iterate**. Start with 200 iterations.

- Once Fluent has stopped iterating, we can post-process the data of our interest.

- We can use **Display > Contours**. and view contour of velocity, pressure etc.